The Plant Cell, Vol. 26: 3569–3588, September 2014, www.plantcell.org

ABCG Transporters Are Required for Suberin and Pollen Wall Extracellular Barriers in *Arabidopsis*[C][W]

Vandana Yadav,[a] Isabel Molina,[b] Kosala Ranathunge,[c] Indira Queralta Castillo,[b] Steven J. Rothstein,[c] and Jason W. Reed[a,1]

[a] Department of Biology, University of North Carolina at Chapel Hill, Chapel Hill, North Carolina 27599-3280
[b] Department of Biology, Algoma University, Sault Ste Marie, Ontario P6A 2G4, Canada
[c] Department of Molecular and Cellular Biology, University of Guelph, Guelph, Ontario N1G 2W1, Canada

Effective regulation of water balance in plants requires localized extracellular barriers that control water and solute movement. We describe a clade of five *Arabidopsis thaliana* ABCG half-transporters that are required for synthesis of an effective suberin barrier in roots and seed coats (ABCG2, ABCG6, and ABCG20) and for synthesis of an intact pollen wall (ABCG1 and ABCG16). Seed coats of *abcg2 abcg6 abcg20* triple mutant plants had increased permeability to tetrazolium red and decreased suberin content. The root system of triple mutant plants was more permeable to water and salts in a zone complementary to that affected by the Casparian strip. Suberin of mutant roots and seed coats had distorted lamellar structure and reduced proportions of aliphatic components. Root wax from the mutant was deficient in alkylhydroxycinnamate esters. These mutant plants also had few lateral roots and precocious secondary growth in primary roots. *abcg1 abcg16* double mutants defective in the other two members of the clade had pollen with defects in the nexine layer of the tapetum-derived exine pollen wall and in the pollen-derived intine layer. Mutant pollen collapsed at the time of anther desiccation. These mutants reveal transport requirements for barrier synthesis as well as physiological and developmental consequences of barrier deficiency.

INTRODUCTION

Correct regulation of water content is essential for plant metabolism, nutrient transport, and growth. Plants adjust to changes in water availability with both physiological responses, such as guard cell opening and closing, and with developmental responses, such as changes in root system architecture (Comas et al., 2013). Several extracellular polymers, including suberin, lignin, and cutin, act as barriers that help plants to control internal water and ion fluxes, limit desiccation, and protect against pathogen attack (Nawrath et al., 2013).

Suberin is deposited adjacent to cell walls around endodermal, exodermal, and peridermal cells of roots and tubers (as in potato [*Solanum tuberosum*] tuber skin), in tree bark (as in cork), in seed coats, at organ abscission zones, and at wound healing sites (Schreiber, 2010; Beisson et al., 2012). Suberin is mostly composed of ester-linked glycerol, very-long-chain fatty acids, dicarboxylic acids, alcohols, hydroxy fatty acids, and ferulic acid. Genes encoding enzymes that synthesize many of these components have been identified in *Arabidopsis thaliana* and potato (Beisson et al., 2012). *Arabidopsis* mutants in these genes make reduced amounts of suberin and/or suberin of altered composition. Some suberin biosynthesis mutants have physiological phenotypes including increased root system hydraulic conductivity, increased seed coat permeability, and seed germination sensitivity to abscisic acid (ABA) (Beisson et al., 2007; Ranathunge and Schreiber, 2011). By transmission electron microscopy (TEM), suberin has a lamellar structure seen as alternating light and dark bands, which may correspond to domains of aliphatic and aromatic components, respectively (Schmutz et al., 1996; Bernards, 2002). However, some plants with defects in aliphatic suberin components had suberin that lacked the dark lamellae (Lee et al., 2009; Molina et al., 2009; Serra et al., 2009), whereas plants having suberin with reduced ferulic acid retained the alternating light and dark bands (Molina et al., 2009; Serra et al., 2010). The mechanisms by which suberin subunits are exported and polymerized are not known.

The suberin precursor biosynthesis genes *GLYCEROL-3-PHOSPHATE ACYL TRANSFERASE5* (*GPAT5*), *FATTY ACID REDUCTASE1* (*FAR1*), *FAR4*, *FAR5*, *CYTOCHROME P450 86A1* (*CYP86A1*)/*HORST*, *CYP86B1*, and *ALIPHATIC SUBERIN FERULOYL TRANSFERASE* (*ASFT*) are each expressed in the maturing root endodermis; several of them can be induced by the stress hormone ABA, salt, or wounding (Beisson et al., 2007; Höfer et al., 2008; Compagnon et al., 2009; Molina et al., 2009; Domergue et al., 2010); and growth on medium containing NaCl increases suberin production (Geng et al., 2013). In addition, the *enhanced suberin1* (*esb1*) and *casp1-1 casp3-1* mutants had a primary defect in formation of the Casparian strip lignin barrier around root endodermal cells, but also had increased suberin deposition in roots (Baxter et al., 2009; Hosmani et al., 2013). The increased suberin production in these mutants suggests the existence of a regulatory mechanism that may compensate for decreased Casparian strip function. The *esb1* mutant root systems

[1] Address correspondence to jreed@email.unc.edu.
The author responsible for distribution of materials integral to the findings presented in this article in accordance with the policy described in the Instructions for Authors (www.plantcell.org) is: Jason W. Reed (jreed@email.unc.edu).
[C] Some figures in this article are displayed in color online but in black and white in the print edition.
[W] Online version contains Web-only data.
www.plantcell.org/cgi/doi/10.1105/tpc.114.129049

have lower solute permeability than do wild-type root systems, probably as a result of their increased suberin content (Ranathunge and Schreiber, 2011).

ATP binding cassette (ABC) transporter proteins are found in both prokaryotes and eukaryotes and pump diverse substrates across membranes using energy from ATP hydrolysis (Higgins and Linton, 2004). Canonical ABC transporters have two repeats each of a transmembrane domain with about six transmembrane helices often conferring substrate specificity and a cytoplasmic ATPase domain. ABC half-transporters have just one of each domain and must form homo- or heterodimers for their transport activity. *Arabidopsis* has ~130 ABC transporters that fall into several clades (Sánchez-Fernández et al., 2001; Verrier et al., 2008). Among these, the ABCG clade is the largest and includes both full-length and half-length transporters.

Several plant ABCG proteins are known or suspected to contribute to synthesis of extracellular barriers. *Arabidopsis* DESPERADO/WBC11/ABCG11 and ABCG12/CER5 are required in the shoot epidermis to transport lipid precursors for cutin and wax biosynthesis (Pighin et al., 2004; Bird et al., 2007; Luo et al., 2007; Panikashvili et al., 2007). These two half-transporters can form heterodimers, and ABCG11 can also homodimerize (McFarlane et al., 2010). *ABCG11* is induced by salt, ABA, and wounding and also affects suberin deposition in roots (Panikashvili et al., 2010). ABCG13 is closely related to ABCG11 and ABCG12 and contributes to cutin formation in flowers (Panikashvili et al., 2011). The full-length transporter ABCG32/PEC1 is required for hydroxylated fatty acid incorporation in the cuticular layer of the cell wall in leaves and flowers (Bessire et al., 2011). ABCG29 exports monolignols required for lignin biosynthesis (Alejandro et al., 2012). Other ABCG transporters are required for pollen exine formation in *Arabidopsis* or rice (*Oryza sativa*; Quilichini et al., 2010; Kuromori et al., 2011; Qin et al., 2013). ABCG9 and ABCG14 can also dimerize with ABCG11, and these as well as ABCG31 affect sterol ester levels in vegetative tissues or on pollen (Le Hir et al., 2013; Choi et al., 2014). In addition, several ABCG proteins are required to transport the hormones ABA, indole-3-butyric acid, strigolactone, or *trans*-zeatin (Strader and Bartel, 2009; Kang et al., 2010; Kuromori et al., 2010; Ruzicka et al., 2010; Kretzschmar et al., 2012; Ko et al., 2014; Zhang et al., 2014) or to transport an unknown substrate required for symbiotic mycorrhizal arbuscule development (Zhang et al., 2010).

We have identified a clade of *Arabidopsis* ABCG half-transporters that are coexpressed with several known suberin biosynthesis genes. A triple mutant deficient in three of these, ABCG2, ABCG6, and ABCG20, had defective suberin lamellar structure and increased seed coat and root system permeability attributable to decreased barrier function. It also had altered root system architecture suggestive of activated stress responses. Two additional proteins in the clade, ABCG1 and ABCG16, were required for pollen wall integrity.

RESULTS

A Clade of ABCG Transporters Is Coexpressed with Suberin Biosynthesis Genes

ABCG1, ABCG2, ABCG6, ABCG16, and ABCG20 proteins form a clade of five ABCG half-transporters (Figure 1A; Supplemental Data Set 1 and Supplemental Figure 1). After transient expression in tobacco (*Nicotiana benthamiana*) leaves, ABCG1:GFP, ABCG2:GFP, ABCG6:GFP, ABCG16:GFP, and ABCG20:GFP protein fusions each colocalized with staining of the plasma membrane marker dye FM4-64 (Supplemental Figure 2), suggesting that they act at the plasma membrane. Based on the ATTED-II and Aranet databases of global gene expression data (Lee et al., 2010; Obayashi et al., 2014) and on a translatome data set of several root and shoot tissues (Mustroph et al., 2009), *ABCG2*, *ABCG6*, *ABCG16*, and *ABCG20* genes are coexpressed with known suberin biosynthesis genes, such as *GPAT5*, *FAR1*, *FAR4*, *FAR5*, *CYP86A1/HORST*, *CYP86B1*, and *ASFT*. Translatome data of different cell types in roots and shoots confirm that *ABCG2*, *ABCG6*, and *ABCG20* expression are particularly enriched in root endodermis (Mustroph et al., 2009) (Supplemental Data Set 2).

X-Gluc staining of plant lines carrying P_{ABCGx}*:GUS* promoter:reporter fusions revealed spatial expression patterns. Five-day-old seedlings of *ABCG1*, *ABCG2*, *ABCG6*, and *ABCG16* reporter lines had X-Gluc staining at the root-shoot junction (Supplemental Figure 3A). Fifteen-day-old seedlings carrying each of the fusions had X-Gluc staining in the endodermal layer of roots (Figure 1B). Endodermal staining only appeared starting in the maturation zone of the root above the meristem. For *ABCG6* and *ABCG20* reporters, X-Gluc staining was also observed in the outer periderm of roots of six-week-old soil-grown plants (Supplemental Figure 3E). All five reporter lines also had expression in anthers and/or in maturing pollen grains (Figures 1C and 1D; Supplemental Figures 3C and 3D). For *ABCG1*, *ABCG2*, and *ABCG16* reporters, anther staining appeared strongest in the tapetal layer (Figure 1D). X-Gluc staining of P_{ABCG20}*:GUS* plants was generally weaker than the others and appeared at a later stage in anthers. P_{ABCG1}*:GUS* was also expressed in the shoot meristematic region, in leaf hydathodes, and in the style (Supplemental Figure 3B). Quantitative RT-PCR assays confirmed much higher expression of each of these genes in roots than in vegetative shoots (Supplemental Figure 4B). In addition, available global gene expression data indicate that all five genes are expressed in developing seed coats (Le et al., 2010; Supplemental Figure 5). These results suggest that these *ABCG* genes act in the maturing root endodermis, in developing anthers and pollen, and in seed coats.

Four-hour treatments of seedlings with any of several hormones increased transcript levels of some of these genes (Figure 2A). ABA increased levels of all five genes, with the greatest effect on *ABCG6* and *ABCG16*; the auxin indole-3-acetic acid (IAA) increased *ABCG6*, *ABCG16*, and *ABCG20* levels; the gibberellin GA_3 increased *ABCG6* level; and the auxin transport inhibitor *N*-1-naphthylphthalamic acid induced *ABCG6*. For P_{ABCG6}*:GUS* and P_{ABCG16}*:GUS* fusions, Fluridone, which inhibits ABA biosynthesis, decreased root staining, and ABA restored staining in the presence of Fluridone (Supplemental Figure 4A). These data indicate that endogenous ABA likely contributes to expression of these genes in root endodermis. In addition, wounding of leaves of 3-week-old plants induced P_{ABCG1}*:GUS*, P_{ABCG2}*:GUS*, P_{ABCG6}*:GUS*, P_{ABCG16}*:GUS*, and (very weakly) P_{ABCG20}*:GUS* within 48 h (Supplemental Figure 3F). Lastly, growth on medium with added mannitol to induce osmotic stress increased root expression of *ABCG2*, *ABCG6*, *ABCG16*, and *ABCG20*, as well as the suberin

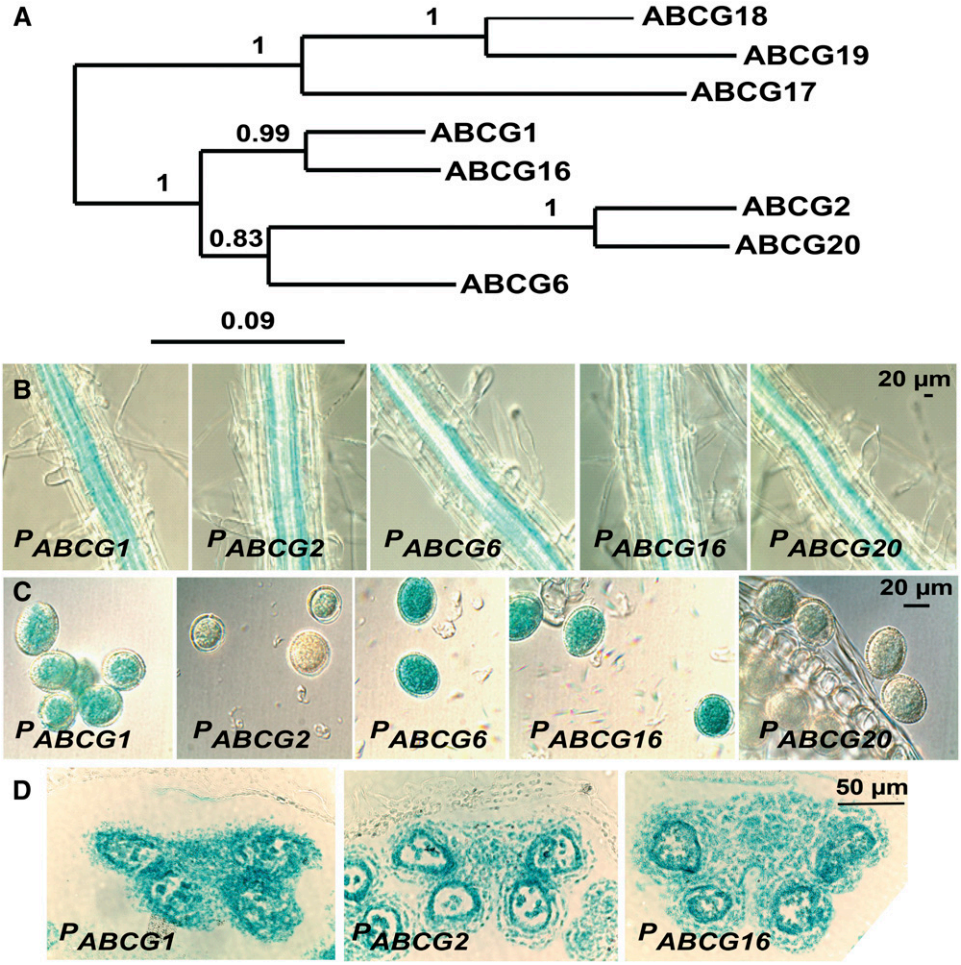

Figure 1. Phylogeny of ABCG Proteins and P_{ABCG}:*GUS* Expression in *Arabidopsis*.

(A) Maximum likelihood phylogenetic tree of *Arabidopsis* ABCG proteins studied here. Numbers at nodes indicate bootstrap estimations of clade support. Scale bar indicates number of mutations per site.

(B) and **(C)** X-Gluc staining of *ABCG1*, *ABCG2*, *ABCG6*, *ABCG16*, and *ABCG20* promoter:GUS reporter lines in root endodermis **(B)** and in pollen **(C)**. Pollen is from stage 12 closed buds just before flower opening (P_{ABCG2}:*GUS* and P_{ABCG16}:*GUS*) or from stage 13 open flowers (P_{ABCG1}:*GUS*, P_{ABCG6}:*GUS*, and P_{ABCG20}:*GUS*). Bars = 20 µm.

(D) X-Gluc staining of anther cross sections. Bar = 50 µm.

biosynthesis genes *GPAT5* and *CYP86B1* (Supplemental Figure 4C). Exogenous NaCl also increases expression in wild-type roots of *ABCG1*, *ABCG6*, *ABCG16*, and *ABCG20* and of several known suberin biosynthesis genes (Geng et al., 2013) (Supplemental Data Set 3). Salt increased expression of some of these genes in endodermis and also in cortex or stele cells.

Taken together, the overlapping expression patterns and similar ABA, mannitol, salt, and wound inducibility of these *ABCG* genes with known suberin biosynthesis genes suggest that they might contribute to suberin deposition.

ABCG2, ABCG6, and ABCG20 Contribute to Suberin Function

To determine physiological functions of these transporters, we characterized effects of two T-DNA insertion alleles in each gene (Supplemental Figure 6A). *abcg1-1*, *abcg2-1*, and the *abcg16* and *abcg20* alleles each had insertions that interrupt the protein coding sequence and are therefore expected to be null alleles. Of the alleles that did not interrupt the coding sequence, the two *ABCG6* alleles had insertions in the promoter or 5′ untranslated region (UTR) and had extremely low expression levels (Supplemental Figure 6B). Insertion *abcg1-2* fell in the 5′ UTR, and *abcg2-2* fell in the 3′ UTR and these each reduced transcript level to ~20% of the wild-type level (Supplemental Figure 6B). As described below, the *abcg1-1* and *abcg1-2* mutations each conferred similar phenotypes in combination with *abcg16* mutations, suggesting that both are strong alleles, whereas the *abcg2-2* allele caused weaker phenotypes than did *abcg2-1*. Thus, most of these mutations are likely to be null except for *abcg2-2*, which may be hypomorphic. As single mutants did not have noticeable phenotypes, we generated several double and triple mutants. We describe in detail

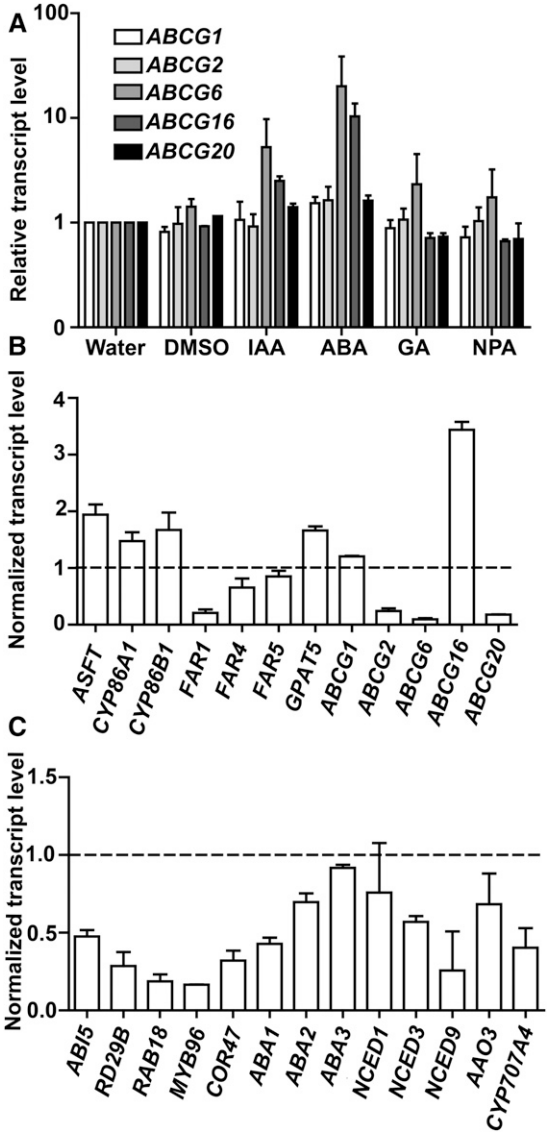

Figure 2. Transcript Levels of *ABCG* Genes in Wild-Type Seedlings and Transcript Levels of Suberin Biosynthesis Genes and ABA-Responsive Genes in *abcg2-1 abcg6-1 abcg20-1* Mutant Roots.

(A) *ABCG1*, *ABCG2*, *ABCG6*, *ABCG16*, and *ABCG20* transcript levels after treatment of 7-d-old wild-type seedlings with 10 μM IAA, ABA, gibberellin A_3 (GA), or *N*-1-naphthylphthalamic acid (NPA) for 4 h, relative to levels in water-treated seedlings.
(B) Transcript levels of suberin biosynthesis and *ABCG* genes in 10-d-old *abcg2-1 abcg6-1 abcg20-1* seedling roots, relative to wild-type levels.
(C) Transcript levels of ABA responsive and ABA biosynthesis genes in 10-d-old *abcg2-1 abcg6-1 abcg20-1* mutant roots, relative to wild-type levels. Transcript levels were normalized to *UBQ10*.
For **(A)** to **(C)**, data shown are means of two biological replicates ±SD.

phenotypes caused by combinations of mutations within each of the two subclades (1) *ABCG2*, *ABCG6*, and *ABCG20*, and (2) *ABCG1* and *ABCG16*.

The *abcg2-1 abcg6-1 abcg20-1* triple mutant had several phenotypes in common with previously described suberin-deficient mutants. It produced darkly colored seeds that had increased permeability to the cationic dye tetrazolium red (Figures 3A and 3B; Supplemental Figure 7A). Although *abcg2-1*, *abcg6-1*, and *abcg20-1* single mutant seeds each had similar seed coat permeability as the wild type in this assay, all three double mutant combinations had increased permeability, with seeds of *abcg2-1 abcg20-1* staining almost as darkly as did *abcg2-1 abcg6-1 abcg20-1* seeds (Figure 3A). Triple mutant seeds were also more sensitive than were wild-type seeds to inhibition of germination by ABA (Figure 3C). A genomic *ABCG2* gene construct could rescue the seed coat permeability defect of the *abcg2-1 abcg6-1 abcg20-1* triple mutant, as well as root phenotypes described below (Supplemental Figure 8). A second independent triple mutant using alternate alleles, *abcg2-2 abcg6-2 abcg20-2*, also had increased seed coat permeability (Supplemental Figure 7B), although this phenotype was weaker than for the *abcg2-1 abcg6-1 abcg20-1* triple mutant, probably because the *abcg2-2* allele is not null. For further analyses, we focused on the *abcg2-1 abcg6-1 abcg20-1* triple mutant.

Root systems of the *abcg2-1 abcg6-1 abcg20-1* triple mutant were more permeable to water than were wild-type root systems. Both hydrostatic hydraulic conductivity (Lp_{hy}, driven by a hydrostatic pressure gradient) and osmotic hydraulic conductivity (Lp_{os}, driven by an osmotic pressure gradient) were about 2-fold higher in mutant than in wild-type root systems (Figure 4A). The Lp_{hy}/Lp_{os} ratios were close to one for both genotypes, indicating a relatively greater symplastic than apoplastic water flow, as for the *horst/cyp86A1* suberin-deficient mutant (Ranathunge and Schreiber, 2011). Similarly, solute permeability (P_{sr}) to NaCl and KNO_3 salts was ~2.5-fold higher in *abcg2-1 abcg6-1 abcg20-1* triple mutant roots than in wild-type roots (Figure 4B).

The Casparian Strip and Suberin Mediate Endodermal Permeability in Different Portions of the Root

The endodermis synthesizes both suberin and a Casparian strip composed of lignin, which serves as a barrier to apoplastic solute movement (Steudle and Peterson, 1998). The Casparian strip appeared intact in *abcg2-1 abcg6-1 abcg20-1* roots by TEM (Figure 4C). We assessed whether the Casparian strip was functional in our plants by assaying root permeability to propidium iodide (PI). Similarly to previous reports (Naseer et al., 2012; Hosmani et al., 2013), PI could enter the central stele of the young portion of 7-d-old wild-type roots up to ~13 cells above the root meristem and could enter the central stele of the Casparian-strip-deficient *esb1-1* mutant up to ~26 cells above the meristem (Figures 4D to 4F). In these two cases, the stele in the older parts of the root 30 or more cells above the meristem did not stain with PI. Similarly as in wild-type roots, PI was blocked from entering the stele of *abcg2-1 abcg6-1 abcg20-1* roots starting 13 cells above the meristem (Figures 4D and 4F). However, in older portions of *abcg2-1 abcg6-1 abcg20-1* roots above 37 cells above the meristem, PI stained the endodermis and central stele (Figure 4E). Similarly, the suberin-deficient plants *gpat5-2* and P_{CASP1}*:CDEF1* (Beisson et al., 2007; Naseer et al., 2012) had an intact barrier to PI movement in the young part of the root but were deficient in excluding PI from the stele of the older part of the root (Supplemental Figure 9A). In the absence of PI, no red fluorescence was observed in the central stele of

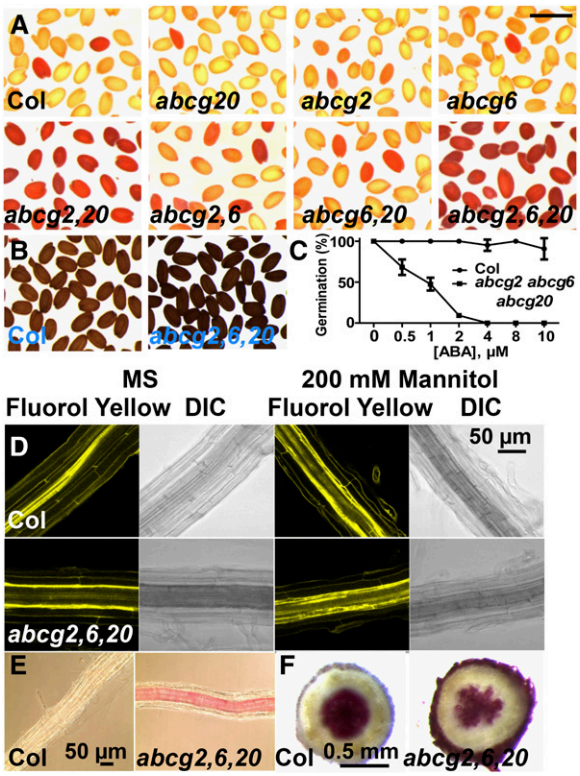

Figure 3. *abcg2-1 abcg6-1 abcg20-1* Mutant Seed Phenotypes and Suberin Staining in Roots.

(A) Tetrazolium staining of seeds of indicated genotypes for 24 h. Seeds are from single, double, and triple mutant combinations of *abcg2-1*, *abcg6-1*, and *abcg20-1* alleles. Bar = 1 mm.

(B) Seed color of Col and *abcg2-1 abcg6-1 abcg20-1*.

(C) Effect of indicated concentrations of ABA on germination of Col and *abcg2-1 abcg6-1 abcg20-1* seeds. Seeds in which the root tip had emerged through the seed coat 7 d after plating were scored as germinated. Data shown are means of two biological replicates ±SD ($n > 50$).

(D) Fluorol Yellow staining of Col and *abcg2-1 abcg6-1 abcg20-1* roots. Seedlings of indicated genotypes were grown on MS for 7 d and then transferred to fresh plates with or without 200 mM mannitol for another 7 d. DIC, differential interference contrast. Bar = 50 µm.

(E) and **(F)** Phloroglucinol staining of roots of 10-d-old **(E)** and 1-month-old **(F)** Col and *abcg2-1 abcg6-1 abcg20-1* plants. Bars = 50 µm in **(E)** and 0.5 mm in **(F)**.

mature *abcg2-1 abcg6-1 abcg20-1* mutant roots, indicating that the red fluorescent signal arose from PI and not from autofluorescence (Supplemental Figure 9B). These results indicate that the Casparian strip is intact and functional in the younger portion (13 to 27 cells above the meristem) of *abcg2-1 abcg6-1 abcg20-1* triple mutant roots, as in other suberin-deficient plants (Naseer et al., 2012). In contrast, in older parts of the root above 37 cells above the meristem, the ABCG transporters and suberin are required to form an endodermal barrier, whereas the Casparian strip lignin band is not.

abcg2-1 abcg6-1 abcg20-1 Plants Produce Suberin with Altered Structure

These physiological phenotypes indicate that *abcg2-1 abcg6-1 abcg20-1* roots have decreased suberin barrier function. However, roots of 10-d-old *abcg2-1 abcg6-1 abcg20-1* seedlings had higher levels of staining with the fluorescent suberin stain Fluorol Yellow than did wild-type roots. Wild-type roots had background cell wall fluorescence or cross-staining of xylem, but only minimal putative Fluorol Yellow suberin staining at the ends of mature endodermal cells. Consistent with the inducibility of suberin biosynthesis genes by mannitol, wild-type root Fluorol Yellow staining was stronger around endodermal cells of plants grown on medium supplemented with mannitol (Figure 3D). In contrast, *abcg2-1 abcg6-1 abcg20-1* triple mutant roots had intense Fluorol Yellow staining along the entire length of the mature endodermis, both in the absence and presence of mannitol (Figure 3D). *abcg2-2 abcg6-2 abcg20-2* endodermis also had higher Fluorol Yellow staining than did wild-type endodermis, although this was less dramatic than in the *abcg2-1 abcg6-1 abcg20-1* triple mutant (Supplemental Figure 7C). Mature portions of *abcg2-1 abcg6-1 abcg20-1* triple mutant roots also stained more strongly than did wild-type roots with Sudan Red, another suberin stain (Supplemental Figure 4D). The endodermis and stele of *abcg2-1 abcg6-1 abcg20-1* triple mutant roots also had greater autofluorescence (Figure 4E; Supplemental Figure 8) and greater staining with the lignin stain phloroglucinol (Figure 3E). The periderm of 1-month-old triple mutant roots stained more strongly with phloroglucinol than did wild-type roots (Figure 3F). This may indicate increased accumulation of aromatic lignin and/or suberin components in the stele and periderm of mutant roots.

Increased suberin deposition in the *abcg2-1 abcg6-1 abcg20-1* mutant root was surprising in light of the increased permeability of mutant roots and seed coats. We therefore analyzed the structure and composition of suberin in the *abcg2-1 abcg6-1 abcg20-1* triple mutant. TEM of the mature zone of 10-d-old wild-type seedling roots (1.5 mm below the root-shoot junction) revealed continuous suberin lamellae on the internal face of endodermal cells between the plasma membrane and primary cell wall. These had alternating light- and dark-staining bands, with adjacent dark bands spaced ~10 to 12 nm apart (Figures 5E and 5G). In contrast, mutant endodermal cells were surrounded by light-staining material that only occasionally had a few short and discontinuous dark lamellae (Figures 5F and 5H). This layer in the mutant often appeared thicker than the suberin lamellae around wild-type endodermal cells. In the mutant, similar light-staining material was also present adjacent to pericycle cells interior to the endodermal cells, suggesting that the mutant may have begun to form periderm characteristic of mature roots (Gambetta et al., 2013). Lastly, the middle lamella between endodermis and pericycle cells appeared darker in the mutant than in the wild type.

Roots from mature soil-grown wild-type plants that had undergone secondary growth had suberin surrounding the outermost layer of periderm cells at the surface (Supplemental Figures 10C and 10E). The lamellae had similar spacing as those outside endodermis of younger roots (Supplemental Figure 10G). Suberin lamellae could also be distinguished in periderm of *abcg2-1 abcg6-1 abcg20-1* triple mutant roots, but the dark-staining bands

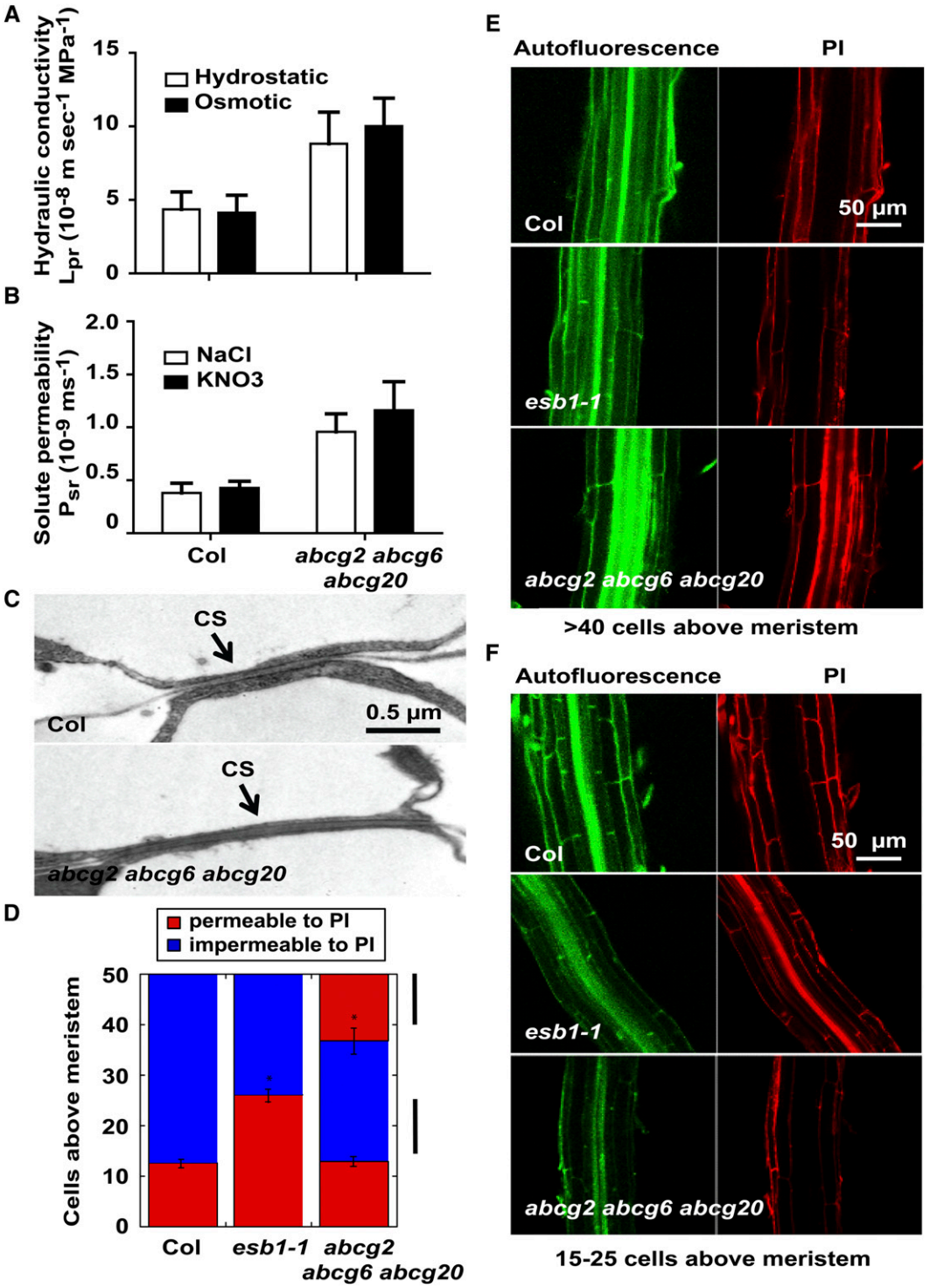

Figure 4. Root Permeability of Col, *esb1-1*, and *abcg2-1 abcg6-1 abcg20-1* Mutants to PI and to Water and Solutes.

(A) and **(B)** Hydrostatic and osmotic hydraulic conductivity **(A)** and salt permeability **(B)** of Col and *abcg2-1 abcg6-1 abcg20-1* mutant root systems. Hydroponically grown roots were used to measure the hydraulic conductivity or salt permeability by root pressure probe at room temperature. Values are means of means (n = 6) ± SD.

(C) TEM of Casparian strip (CS) in Col and *abcg2-1 abcg6-1 abcg20-1* roots sectioned 2 mm above the root tip. Bar = 0.5 µm.

were lighter than those in wild-type roots (Supplemental Figures 10F and 10H). Thus, suberin in the mutant had similarly altered appearance in both the young root endodermis and the mature root periderm. Seed coats of the *abcg2-1 abcg6-1 abcg20-1* triple mutant had similarly decreased lamellar structure (Supplemental Figure 11). As discussed below, the mutant root periderm cells were also smaller than those of wild-type roots (Supplemental Figure 10D). Together with the physiological assays above, these results suggest that suberin of the triple mutant is deficient in components that confer lamellar structure and barrier properties.

abcg2-1 abcg6-1 abcg20-1 Plants Produce Altered Suberin Polyester and Root Wax

We analyzed the abundance of suberin polyester monomers extracted from root periderm of 7-week-old wild-type and triple mutant plants (Figure 6A; Supplemental Figure 12) and from roots of 10-d-old plants, which had not yet undergone significant periderm development and therefore contained mostly endodermal suberin (Supplemental Figure 13). Yields from periderm of wild-type 7-week-old plants were ~6-fold higher than those from endodermis of 10-d-old plants. Consistent with the microscopy and Fluorol Yellow staining results, total suberin aliphatic monomer content per dry weight was ~70% higher in roots of 10-d-old seedlings of *abcg2-1 abcg6-1 abcg20-1* than in wild-type roots and ~3-fold higher in mutant periderm from 7-week-old plants (Figure 6A, inset; Supplemental Figure 13, inset). Compared with suberin from wild-type root periderm, suberin from mutant root periderm had 2-fold or lower relative proportions of 20:0 and 22:0 fatty acids and 22:0 fatty alcohol (1-OH 22:0) and a 33% relative decrease in 18:1 ω-hydroxy fatty acid (Figure 6A). (A 40% decrease in ferulate was not significant at $P < 0.05$.) When normalized to dry weight, only 22:0 fatty acid and 22:0 fatty alcohol were lower in mutant than wild-type samples (Supplemental Figure 12A). Conversely, suberin from mutant root periderm had 2-fold or higher molar proportions of 24:0 fatty acid, 18:0, 20:0, and 22:0 dicarboxylic acids, and 20:0 hydroxy fatty acid. Suberin from 10-d-old triple mutant seedling roots had decreased proportions of ferulate, 22:0 fatty acid, 18:0 and 22:0 fatty alcohols, and 18:2 dicarboxylic acid as well as higher proportions of 18:1 and 22:0 dicarboxylic acids and 20:0 and 22:0 hydroxy fatty acids (Supplemental Figure 13).

We also analyzed periderm suberin composition from roots of 7-week-old single and double mutant plants (Supplemental Figure 14) and from 10-d-old double mutant plants (Supplemental Figure 13). The single and double mutants generally had weaker suberin phenotypes than the triple mutant. Of the single mutants, *abcg2-1* had the largest defect, with lower levels of fatty alcohols than the wild type. The double mutants generally had intermediate levels of most components, with the *abcg2-1 abcg6-1* and *abcg2-1 abcg20-1* double mutants having larger differences from the wild type than the *abcg6-1 abcg20-1* double mutant. Curiously, in 10-d-old plant roots, the *abcg2-1 abcg6-1* and *abcg2-1 abcg20-1* double mutants had proportions of 18:0 and other fatty alcohols that were higher than were recovered from either wild-type or triple mutant roots (Supplemental Figure 13).

In contrast to mutant roots, total suberin polyester monomer content in *abcg2-1 abcg6-1 abcg20-1* seeds was less than half that of wild-type seeds (Figure 6B, inset). This result suggests that the apparent compensatory increase in suberin biosynthesis seen in mutant roots does not occur in seeds. On a molar ratio basis, suberin from mutant seeds had 2-fold or lower amounts of ferulate, 16:0 and 24:0 hydroxy fatty acids, and 22:0 fatty alcohol compared with suberin from wild-type seeds and smaller decreases in 22:0 hydroxy fatty acid and 18:0 fatty alcohol (Figure 6B). However, when normalized to seed weight, suberin from mutant seeds also had lower levels of coumarate, 24:0 fatty acid, 18:2 and 24:0 dicarboxylic acids, and 18:1, 18:2, and 22:0 hydroxy fatty acids (Supplemental Figure 12B). Overall, the most consistent differences from the wild type shared among root and seed coat *abcg2-1 abcg6-1 abcg20-1* suberin were reduced proportions of ferulate, 22:0 alcohol, and 22:0 fatty acid, and increased proportions of saturated 18:0-22:0 dicarboxylic acids.

Root waxes are soluble lipids that can be isolated from roots by a quick chloroform extraction (Li et al., 2007; Kosma et al., 2012). These compounds are not polymerized and may include suberin precursors. We analyzed waxes from roots of 7-week-old wild-type and *abcg2-1 abcg6-1 abcg20-1* mutant plants (Figure 7). In these samples, aromatic acids are present as esters with fatty alcohols. Strikingly, 20:0 and 22:0 alkyl coumarates, 18:0, 20:0, and 22:0 alkyl ferulates, and 18:0, 20:0, and 22:0 alkyl caffeates were all substantially decreased in the triple mutant roots. The largest effects were on alkyl ferulates and alkyl caffeates, most of which were not detected in waxes from the triple mutant. In addition, 20:0 fatty acid and 20:0 fatty alcohol were decreased in the mutant, as well as 29:2 sterol and β C24 monoacyl glycerol. Conversely, several compounds were increased, most notably 18:0 fatty alcohol and, to a lesser extent, 22:0 fatty alcohol. The increased free fatty alcohol content in mutant root wax contrasts with results of suberin monomer analyses and suggest that much of the fatty alcohols recovered from suberin may be incorporated as alkyl ferulates.

abcg2-1 abcg6-1 abcg20-1 Roots Have Altered Expression of Suberin Biosynthesis Genes

To explore the basis for the increased production and altered composition of suberin in *abcg2-1 abcg6-1 abcg20-1* roots, we

Figure 4. (continued).

(D) Portions of roots of 8-d-old seedlings of indicated genotypes that were permeable or impermeable to PI movement into the central stele, mapped by the positions of endodermal cells above the meristem that permitted or impeded penetration of PI. The 0 on the *y* axis represents the boundary between the meristem and the elongation zone. Red bars represent regions that are permeable to PI and blue bars regions that are impermeable to PI, with mean positions of boundaries between these zones ± SD ($n \geq 10$). Asterisk indicates $P < 0.05$ by *t* test compared with wild-type values. Black bars at the right of the graph indicate the zones of mature cells shown in **(E)** (upper bar) and young root cells shown in **(F)** (lower bar).

(E) and **(F)** Representative images showing autofluorescence and PI staining in mature **(E)** or young **(F)** regions of roots of indicated genotypes. Bar = 50 μm.

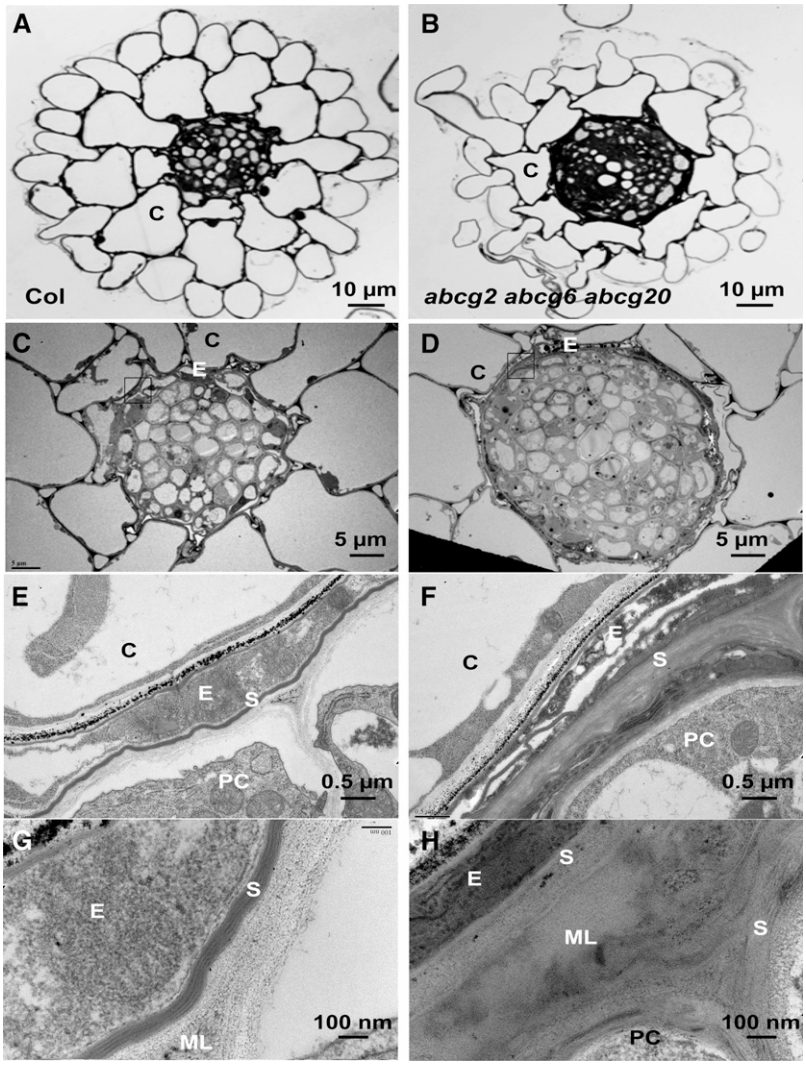

Figure 5. Structure of Col and *abcg2-1 abcg6-1 abcg20-1* Roots.

Ten-day-old seedlings grown on vertically oriented plates were fixed, and the mature region of roots 1 to 1.5 mm below the root-shoot junction were sectioned. C, cortex; X, xylem; PC, pericycle; E, endodermis; ML, middle lamella; S, suberin.
(A) and **(B)** Light microscope images of Col **(A)** and *abcg2-1 abcg6-1 abcg20-1* **(B)** root transverse sections stained with Toluidine blue. Bars = 10 µm.
(C) and **(D)** TEM of Col and *abcg2-1 abcg6-1 abcg20-1* root central stele. Boxed regions indicate regions shown in **(E)** and **(F)**. Bars = 5 µm.
(E) and **(F)** TEM of Col and *abcg2-1 abcg6-1 abcg20-1* endodermal cells. Bars = 0.5 µm.
(G) and **(H)** TEM of Col and *abcg2-1 abcg6-1 abcg20-1* suberin lamellae at higher magnification. Arrows indicate suberin layers. Bars = 100 nm.

assayed expression of several suberin biosynthesis genes. Mutant roots had higher transcript levels of *GPAT5*, *CYP86A1*, *CYP86B1*, and *ASFT* than did wild-type roots (Figure 2B), suggesting that increased expression of these and other biosynthetic genes accounts for higher suberin deposition in the triple mutant. Products of these genes synthesize hydroxy fatty acids (CYP86A1 and CYB86B1) and esterify long-chain fatty acids (GPAT5) and ferulate (ASFT). In contrast, transcripts of *FAR1* and possibly also *FAR4* were decreased in *abcg2-1 abcg6-1 abcg20-1* mutant roots (Figure 2B). FAR1 and FAR4 synthesize primary fatty alcohols that are incorporated into suberin (Domergue et al., 2010; Vishwanath et al., 2013), and decreased expression of *FAR1* and *FAR4* may therefore explain the decreased fatty alcohol contents in the mutant suberin (Figure 6A). In addition, *ABCG16* was overexpressed in *abcg2-1 abcg6-1 abcg20-1* roots (Figure 2B), suggesting that it may compensate in part for loss of ABCG2, ABCG6, and ABCG20.

Increased suberin biosynthesis gene expression raises the possibility that ABA responses might be increased in *abcg2-1 abcg6-1 abcg20-1* roots. However, several genes that encode proteins in ABA biosynthesis (*NCED1*, *NCED3*, *NCED9*, *ABA2*, *ABA3*, and *AAO3*) or ABA catabolism (*CYP707A4*), as well as several ABA-responsive genes (*RAB18*, *COR47*, *RD29B*, *MYB96*, and *ABI5*), were either expressed at wild-type levels or underexpressed in *abcg2-1 abcg6-1 abcg20-1* roots (Figure 2C). These

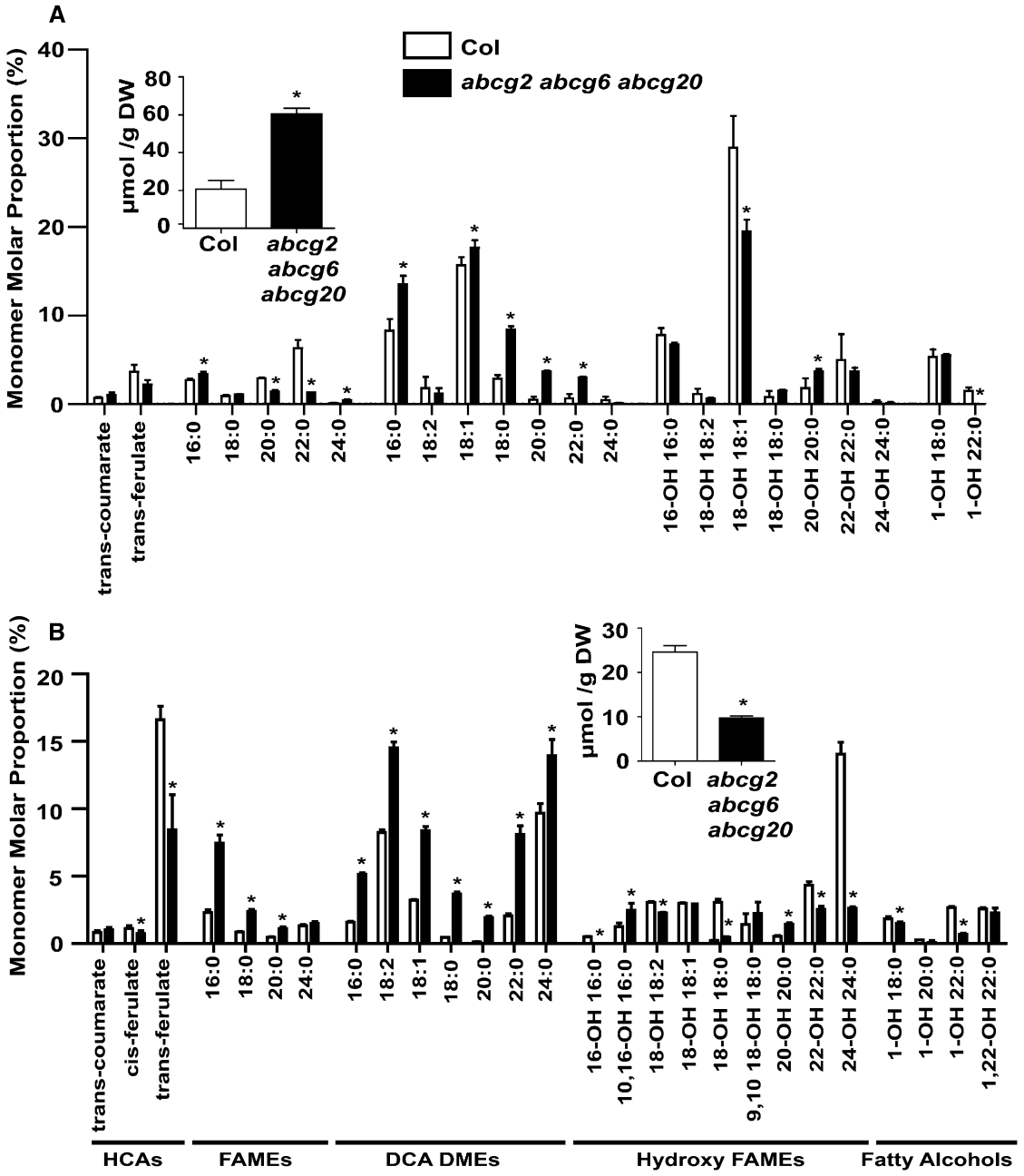

Figure 6. Suberin Monomer Composition of Col and *abcg2-1 abcg6-1 abcg20-1* Roots and Seeds.

(A) Root suberin monomers.

(B) Seed suberin monomers.

Data are expressed as molar percentage of all monomers collected. Insets: total amount of suberin monomers recovered, in µmoles per gram of dry weight. Data are means from three (root) or four (seed) replicate samples ±SD. Asterisk indicates $P < 0.05$ by *t* test.

results suggest that mutant roots do not have a sustained increase in ABA response. P_{SCR}:*abi1-1* seedlings, which have decreased ABA response specifically in the endodermis (Duan et al., 2013), had increased Fluorol Yellow staining around the endodermis after growth on mannitol, although this appeared weaker than the effect in wild-type seedlings (Supplemental Figure 4E; Figure 3D). These results suggest that ABA may contribute to induction of suberin biosynthesis but that signals other than ABA can also stimulate suberin biosynthesis under osmotic stress or in the mutant roots.

Altered Growth of *abcg2-1 abcg6-1 abcg20-1* Plants

Microscopy of maturing roots of 10-d-old seedlings revealed that the central stele of *abcg2-1 abcg6-1 abcg20-1* roots was

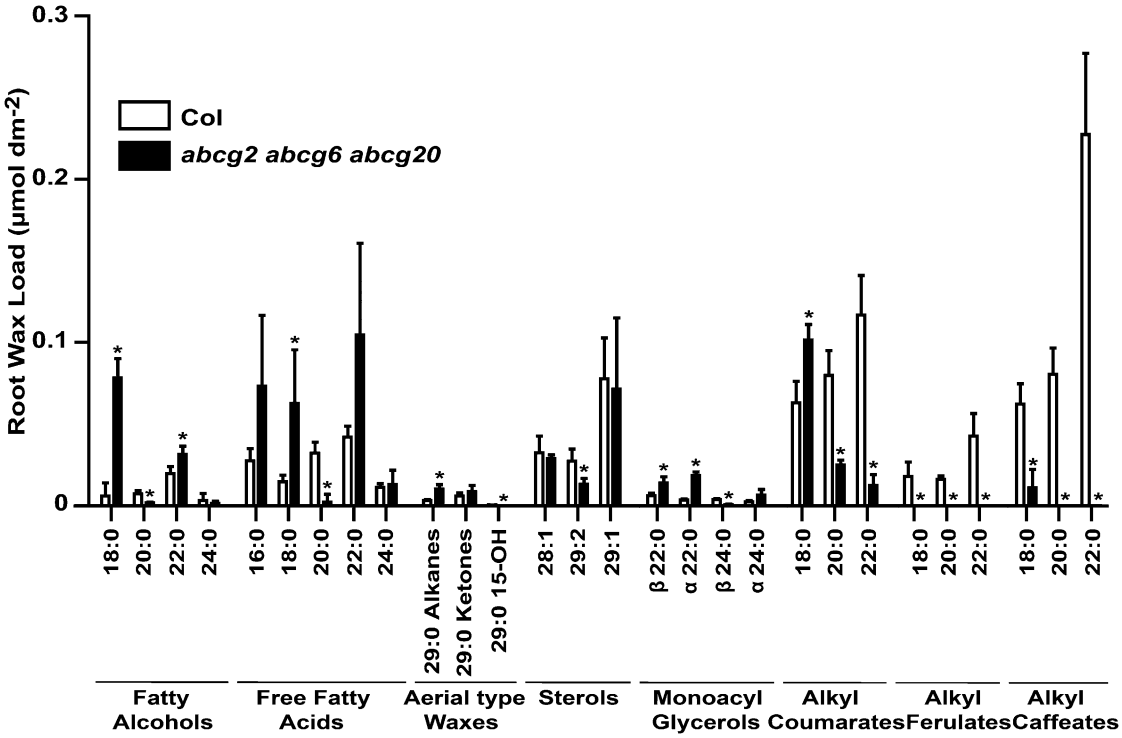

Figure 7. Root Wax Composition from Col and *abcg2-1 abcg6-1 abcg20-1* Roots.

Data are means from four replicate samples ±SD. Asterisk indicates $P < 0.05$ by *t* test.

broader and had more cells than did the stele of wild-type roots and that the triple mutant also had slightly deformed epidermal and cortical cells (Figures 5A to 5D), suggesting that secondary growth had begun precociously in the mutant. In mature roots of soil-grown plants, mutant periderm had smaller cells that appeared less regularly packed than corresponding cells in wild-type plants, and many small cells appeared to be sloughing off from the root surface (Supplemental Figures 10A, 10B, 10E, and 10F). Cells interior to the periderm also appeared less organized than in the wild type. These observations suggest that the phellogen cells, which give rise to periderm, may have continued to divide at a stage when wild-type phellogen cells had differentiated and that the mutant cells may be less adherent than wild-type cells.

The *abcg2-1 abcg6-1 abcg20-1* seedlings also had fewer emerged lateral roots and fewer visible lateral root primordia than did wild-type seedlings (Figures 8A and 8B; Supplemental Figures 15B and 15C). Single and double mutants had intermediate numbers of lateral roots (Supplemental Figure 15B). *abcg2-2 abcg6-2 abcg20-2* triple mutants, as well as the suberin-deficient mutants *gpat5-1*, *asft-1*, and *cyp86a1-2*, also had fewer lateral roots than did wild-type plants, although they had more lateral roots than did *abcg2-1 abcg6-1 abcg20-1* seedlings (Supplemental Figure 15B and D). Although *abcg2-1 abcg6-1 abcg20-1* mutant plants had fewer lateral roots than did wild-type plants, they often had adventitious roots that grew from the base of the hypocotyl, and these adventitious roots often grew as long as the primary root (Figures 8A and 8C; Supplemental Figure 15A). When incorporated into the growth medium, exogenous IAA increased the numbers of emerged lateral roots in both wild-type and triple mutant seedlings, to similar numbers at the highest concentration tested (Figure 8B), although under these conditions these lateral roots remained quite short (Supplemental Figures 15E and 15F). Although cotyledons and leaves initially appeared similar in wild-type and *abcg2-1 abcg6-1 abcg20-1* seedlings, after growth for more than 7 d, triple mutant plants also had smaller leaves than did wild-type plants (Supplemental Figures 15A and 16).

Altered water balance in *abcg2-1 abcg6-1 abcg20-1* plants might cause the changes seen in nonendodermal root cell types, such as the stele and pericycle, and the decreased shoot growth. We assessed the responses of wild-type and *abcg2-1 abcg6-1 abcg20-1* plants to decreased water availability by growing them on medium with added mannitol. Mannitol is known to decrease lateral root formation or elongation (Xiong et al., 2006; Macgregor et al., 2008; Zolla et al., 2010). Under our conditions, mannitol decreased both root elongation and shoot growth (Figures 8D and 8E). For root and possibly leaf growth, the *abcg2-1 abcg6-1 abcg20-1* mutant appeared more sensitive to mannitol, indicating that suberin biosynthesis in wild-type plants can contribute to effective osmotic stress tolerance.

ABCG1 and ABCG16 Contribute to Pollen Wall Integrity

ABCG1 and ABCG16 comprise a sister clade to ABCG2, ABCG6, and ABCG20 (Figure 1A). *abcg1 abcg16* double mutants with either of two independent allelic combinations, as well as the

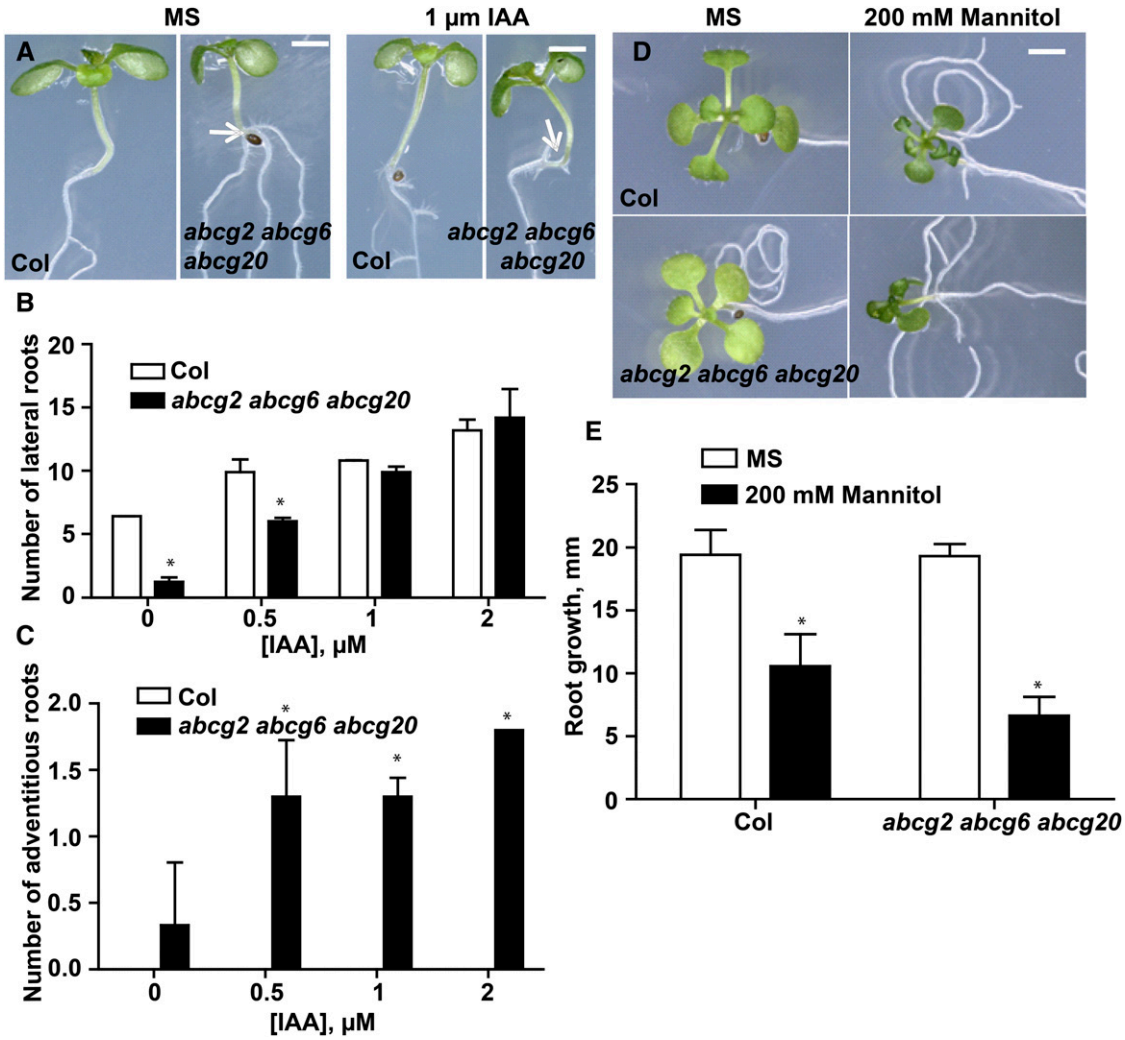

Figure 8. Growth Phenotypes of *abcg2-1 abcg6-1 abcg20-1* Seedlings.

(A) to **(C)** Five-day-old seedlings of Col and *abcg2-1 abcg6-1 abcg20-1* grown on vertically oriented plates were transferred to medium with or without the indicated concentrations of IAA for 1 week.

(A) Appearance of seedlings grown with or without 1 μM IAA. Arrows indicate adventitious roots from the mutant hypocotyl. Bar = 1 mm.

(B) and **(C)** Numbers of visible lateral roots **(B)** and adventitious roots emerged from the hypocotyl **(C)**. Data are means ± SD (n = 5). Asterisk represents $P < 0.05$ by t test.

(D) Seedlings of Col and *abcg2-1 abcg6-1 abcg20-1* were grown on MS for 7 d and then transferred to fresh plates with or without 200 mM mannitol for 2 weeks. Bar = 1 mm.

(E) Root growth of Col and *abcg2-1 abcg6-1 abcg20-1* seedlings grown on MS for 7 d and then transferred onto 200 mM mannitol plates for another 7 d. Asterisk represents $P < 0.05$ by t test.

[See online article for color version of this figure.]

abcg1-1 abcg16-1 abcg20-1 triple mutant, had decreased male fecundity. More than 90% of mature pollen grains of *abcg1 abcg16* plants appeared shriveled (Supplemental Table 1), and *abcg1 abcg16* and *abcg1-1 abcg16-1 abcg20-1* anthers released only a small amount of pollen, most of which was shriveled (Figures 9A and 9E; Supplemental Figures 17A and 17B). At least some of the uncollapsed pollen was apparently viable, as the mutants could be propagated by self-pollination. Among progeny of self-pollinated *ABCG1/abcg1-2 ABCG16/abcg16-2* double heterozygotes, the *abcg1-2 abcg16-2* and other mutant genotypes were recovered at frequencies consistent with a sporophytic defect (Supplemental Table 2). Moreover, sesquimutants homozygous for either *abcg1-2* or *abcg16-2* and heterozygous for the other mutation produced over 80% uncollapsed pollen, a proportion much higher than the 50% that would be expected for a gametophytic effect (Supplemental Table 1).

We analyzed *abcg1-1 abcg16-1 abcg20-1* pollen in more detail. Mutant pollen grains appeared outwardly normal until approximately

one to two flowers before flower opening (flower stage 12), at which point they collapsed (Figures 9E, 10H, and 10J; Supplemental Figure 17C). TEM analyses revealed that at flower stage 11, before the pollen collapse, the cytoplasm of *abcg1-1 abcg16-1 abcg20-1* pollen had shrunk so that the plasma membrane retracted away from the cell wall (Figure 10B). This shrinkage might have occurred during pollen development or during fixation for TEM but was not seen in wild-type pollen (Figure 10A).

Pollen is surrounded by an intine cell wall layer made by the pollen grain and an exine layer rich in the polymer sporopollenin made by the tapetum of the anther (Blackmore et al., 2007). The exine layer has an inner component called nexine or endexine and an outer layer called sexine or ektexine. Developing pollen of the *abcg1-1 abcg16-1 abcg20-1* and *abcg1-2 abcg16-2* mutants stained more brightly with Auromine O than did wild-type pollen, indicating that the sexine layer is present (Figure 9E; Supplemental Figure 17). Moreover, TEM of developing pollen grains revealed that *abcg1-1 abcg16-1 abcg20-1* triple mutant pollen had the characteristic structure of the sexine layer consisting of columns of opaque material (Figures 10A to 10F). At flower stage 12, when the mutant pollen had collapsed, these columns appeared more densely packed than in wild-type pollen (Figures 10G to 10J).

Whereas the sexine layer appeared intact, the narrow electron-dense nexine layer interior to the sexine layer often appeared to stain more lightly or discontinuously in developing mutant pollen than in wild-type pollen (Figures 10C to 10F). The layer appeared intact in mature collapsed mutant pollen (Figures 10I and 10J). These observations suggest that mutant pollen may have a delay in nexine formation or an altered nexine structure. As this layer is a minor component of the exine layer and difficult to isolate, we did not try to assay its chemical composition.

To assess the integrity of the intine layer, we stained wild-type and *abcg1-1 abcg16-1 abcg20-1* mutant pollen with Calcofluor, which binds to oligosaccharides with β-1,3 and β-1,4 glycosyl linkages (Wood, 1980). Whereas wild-type pollen stained evenly with Calcofluor, ~80% of *abcg1-1 abcg16-1 abcg20-1* mutant pollen lacked Calcofluor staining (Figures 9B to 9D). This was true of both immature pollen in anthers of stage 11 flowers and of mature pollen in anthers of stage 12 flowers just before flowers open (Smyth et al., 1990). Similarly, in TEM images, whereas an intine layer was visible in wild-type pollen grains at both immature and mature stages (Figures 10C, 10E, and 10I), this layer was not seen in the mutant pollen (Figures 10D, 10F, and 10J).

DISCUSSION

ABCG Transporters Are Required for Barrier Synthesis

Our results indicate that ABCG2, ABCG6, and ABCG20 transporters together are required to form effective suberin barriers to water and solute movement. Both roots and seed coats of mutants deficient in these transporters had increased permeability, similarly to roots and seed coats of previously described suberin-deficient mutants. The mutant roots did make suberin, but this was structurally altered, suggesting that a specific component or organization is required to form an effective seal. These mutants therefore provide insight into suberin biosynthesis and structural requirements for suberin barrier properties.

Similarly, the closely related transporters ABCG1 and ABCG16 are required for pollen wall integrity. Most pollen from *abcg1 abcg16* mutant plants collapsed at flower stage 12, when wild-type pollen matures and anthers desiccate and release pollen (Wilson et al., 2011). This pollen phenotype was inherited sporophytically and may have arisen from a defect in synthesis of the inner exine layer called nexine or endexine. Strong expression of P_{ABCG1}*:GUS* and P_{ABCG16}*:GUS* fusions in the tapetum are consistent with this interpretation. In addition, the intine layer of *abcg1 abcg16 abcg20* triple mutant pollen was often missing, suggesting that a sporophytic function is required for intine as well as exine synthesis (although the *ABCG* genes were also expressed in pollen). Other workers have also found that nexine defects lead to absence of intine formation and to shriveled pollen (Lou et al., 2014). Mutants with defects in the outer layer of exine, called sexine or ektexine, also have defective pollen that can appear shriveled or abort (Morant et al., 2007; de Azevedo Souza et al., 2009; Quilichini et al., 2010; Dobritsa et al., 2011).

While biochemical studies of exine structure and biosynthesis are challenging (Quilichini et al., 2014), further microscopy studies of early stages of *abcg1 abcg16* mutant anther and pollen development starting at the free microspore stage might help to identify more definitively which wall component is affected and when the defect first appears. Although mature pollen naturally hydrates through the apertures, it may be possible to design pollen permeability assays analogous to those used to characterize effects of suberin deficiency in roots to test whether the mutant pollen has an effective seal against water loss. Alternatively, acetolysis might reveal whether the exine is structurally intact (Ariizumi et al., 2003). If the mutant pollen wall is more permeable or fragile than wild-type pollen, then the root suberin and pollen wall defects may arise from defects in structurally and functionally related barrier molecules.

Both the suberin and pollen wall defects may be incomplete, as all five *ABCG* genes were expressed in root endodermis, in seed coats, and in developing anthers and pollen, and may therefore act partially redundantly in these tissues. While little is known of the detailed composition of nexine, suberin and sporopollenin (comprising both nexine and sexine) each contain polymerized fatty acids and aromatic compounds (Ariizumi and Toriyama, 2011; Beisson et al., 2012; Nawrath et al., 2013). Moreover, lily (*Lilium longiflorum*) nexine is first synthesized as lamellae, and in some plant species mature nexine is lamellar (Dickinson and Heslop-Harrison, 1968; Weber and Ulrich, 2010). Thus, nexine may have a similar structure to suberin. However, the strong phenotypes of *abcg2 abcg6 abcg20* and *abcg1 abcg16* mutants, despite the overlapping expression patterns of all five genes, raise the alternative possibility that proteins in the two subclades have differing substrate preferences. Further characterizations of these transporters may reveal whether this is true and may help to elucidate the composition of the nexine layer of pollen.

ABCG Proteins May Transport Aliphatic Polymer Precursors

That the *abcg2-1 abcg6-1 abcg20-1* mutant roots deposit substantial amounts of permeable suberin suggests that specific

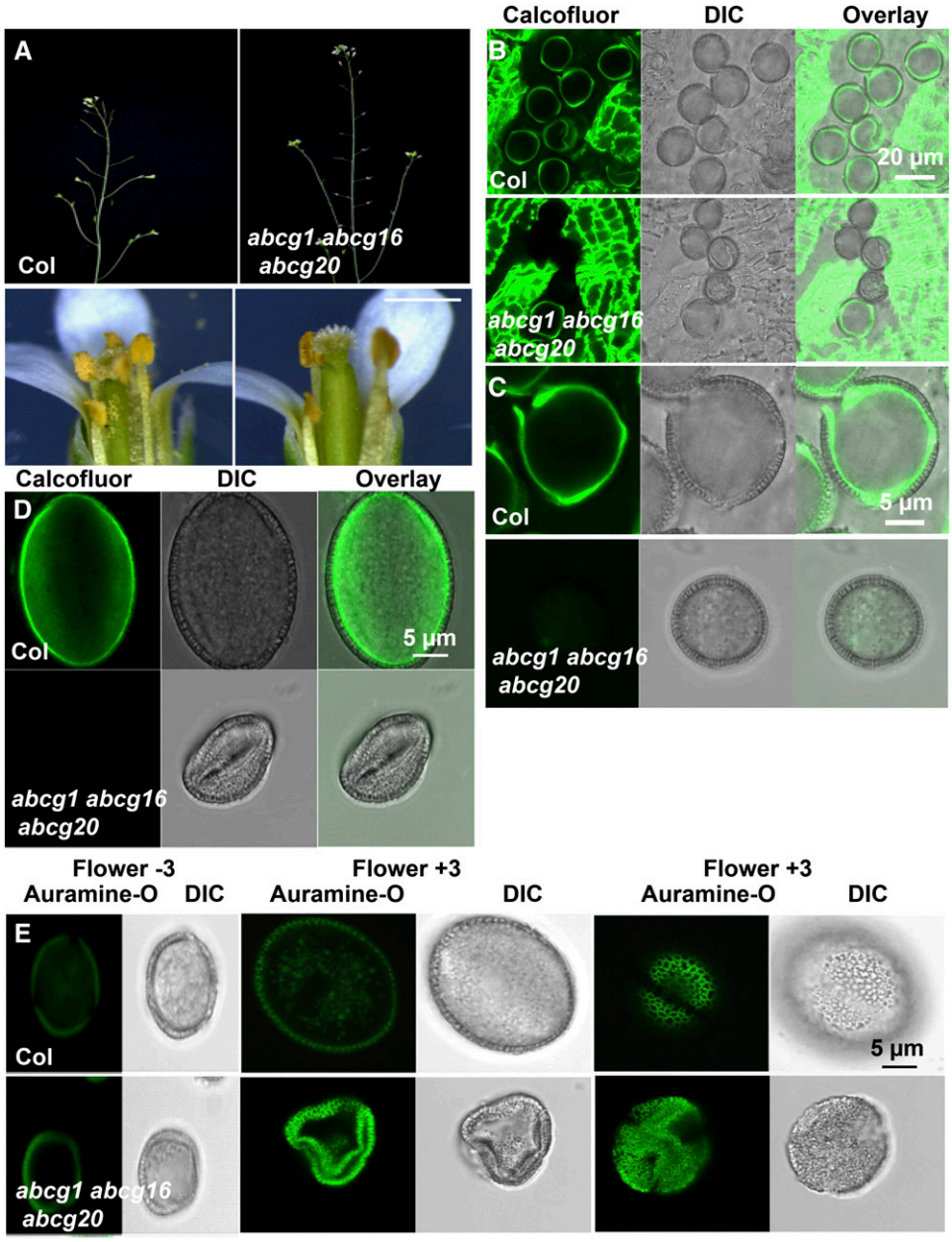

Figure 9. Pollen Phenotypes of Col and *abcg1-1 abcg16-1 abcg20-1* Plants.

(A) Inflorescences and open stage 13 flowers (Smyth et al., 1990).
(B) Calcofluor staining of anthers of stage 11 flowers (three or four flowers before the first open flower).
(C) Calcofluor staining of immature pollen from stage 11 flowers.
(D) Calcofluor staining of mature pollen from stage 13 flowers (the third open flower).
(E) Auramine-O staining of pollen. Flower -3 and Flower +3 indicate immature pollen from stage 11 flowers (the third bud before flower opening) and mature pollen from stage 13 flowers (the third open flower), respectively.
Images in **(B)** to **(E)** were by confocal microscopy. For the mature pollen in **(E)**, medial and surface optical sections are shown. Bars = 20 µm in **(B)** and 5 µm in **(C)** to **(E)**.

chemical components or structural features of suberin underlie its barrier properties. Suberin in roots of the *abcg2-1 abcg6-1 abcg20-1* mutant had decreased proportions of 20:0 and 22:0 fatty acids, 22:0 fatty alcohol, and 18:1 ω-hydroxy fatty acid, raising the possibility that the mutant is deficient in exporting fatty acids or fatty alcohols. Consistent with a possible fatty acid transport defect, rice plants mutant for *OsABCG5/RCN1*, encoding a putative ortholog of the entire clade of *Arabidopsis* ABCG proteins studied here (Yasuno et al., 2009), had root hypodermis suberin with decreased amounts of 28:0 and 30:0 fatty

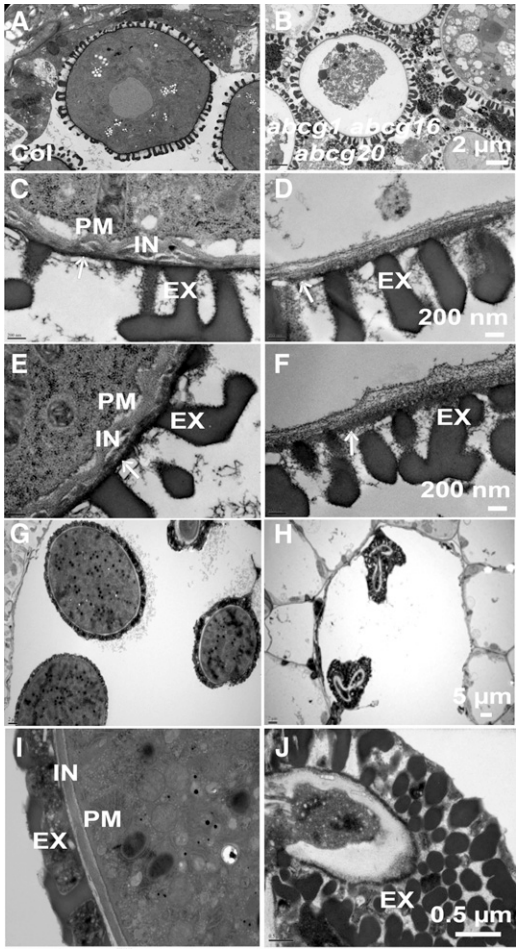

Figure 10. Transmission Electron Microscopy of *abcg1-1 abcg16-1 abcg20-1* Pollen.

(A) to **(F)** Pollen from stage 11 flowers (the third bud before flower opening).
(G) to **(J)** Pollen from stage 12 flowers (the last closed bud before flower opening).
(A), **(C)**, **(E)**, **(G)**, and **(I)** Wild-type pollen.
(B), **(D)**, **(F)**, **(H)**, and **(J)** *abcg1-1 abcg16-1 abcg20-1* pollen.
EX, exine; IN, intine; PM, plasma membrane. Arrows in **(C)** to **(F)** indicate the nexine layer. Bars = 2 µm in **(A)** and **(B)**, 200 nm in **(C)** to **(F)**, 5 µm in **(G)** and **(H)**, and 0.5 µm in **(I)** and **(J)**.

acids, several ω-hydroxyacids, and C16 and C18 diacids (Shiono et al., 2014). By contrast, the *Arabidopsis dso/abcg11* mutant, which is mostly affected in cutin composition, had significant reductions in some suberin components but not in C22:0 acid or alcohol (Panikashvili et al., 2010). Suberin of the *abcg2-1 abcg6-1 abcg20-1* triple mutant root lacked dark lamellae normally seen in TEM images, and other plants with defects in aliphatic components of suberin also make suberin in which these dark bands are disrupted. These include tuber periderm cell walls of potato plants with silenced *CYP86A33*, having suberin deficient in glycerol, C18:1 ω-hydroxyacid, and α,ω-diacid (Serra et al., 2009); root periderm cell walls of *Arabidopsis cyp86A1* mutants having suberin deficient in several fatty acids, hydroxy fatty acids, and diacids (Li et al., 2007; Höfer et al., 2008; Molina et al., 2009); and *Arabidopsis* plants deficient in *KCS20* and *KCS2/DAISY*, encoding 3-ketoacyl CoA synthases required for long-chain fatty acid synthesis (Franke et al., 2009; Lee et al., 2009). Thus, both the chemical analyses and the suberin structure observed by TEM are consistent with a defect in aliphatic components. The substrate(s) that the ABCG proteins actually transport might therefore be fatty acids, fatty alcohols, and/or conjugates of one of these. Mutant seed suberin had almost normal fatty acid content but reduced levels of ferulic acid, fatty alcohols, and hydroxy fatty acids, which suggests that the ABCG proteins may transport hydroxylated precursors.

Analysis of root waxes provided additional insight into the possible substrates of these transporters. Root waxes include compounds that may be precursors of suberin that are not yet polymerized, including several alkylhydroxycinnamates. Waxes from *abcg2-1 abcg6-1 abcg20-1* mutant roots were strikingly deficient in alkyl ferulates and alkyl caffeates and to a lesser degree alkyl coumarates. Intracellular feruloyl-CoA- or caffeoyl-CoA-acyltransferases synthesize these alkylhydroxycinnamates, and defects in these enzymes affect suberin and/or wax composition in both *Arabidopsis* and potato (Gou et al., 2009; Molina et al., 2009; Serra et al., 2010; Kosma et al., 2012). Our data thus suggest that the ABCG proteins may transport alkylhydroxycinnamates, which might in turn cause deficiencies in ferulate, fatty alcohols, and fatty acids in polymerized suberin in the mutant. This scenario suggests that a significant portion of fatty alcohol monomers in polymerized suberin may come from alkylhydroxycinnamates that are exported and polymerized, rather than from exported free fatty alcohols. Similarly, a portion of the bound ferulate in suberin is esterified to fatty alcohols (Gou et al., 2009; Molina et al., 2009; Serra et al., 2010). The *abcg2-1 abcg6-1 abcg20-1* plants appear to have more severe suberin structural defects than do the *asft/hht* and *fact* mutants, which are affected in suberin ferulate or root alkylcaffeates, respectively. It will be interesting in this regard to make higher-order mutants deficient in multiple hydroxycinnamyl-CoA-acyltransferases.

Whatever the primary transport defect may be, the increases in several dicarboxylic acids and hydroxy fatty acids in the mutant root suberin may arise from diversion of biosynthetic precursors toward these products and from compensatory induction of multiple suberin biosynthesis genes. This compensation may be less pronounced in mutant seed coats, which did not have excess suberin monomers. Alternatively, precursor metabolite pools may differ between seed coats and roots. The decreased *FAR1* and *FAR4* expression in the *abcg2-1 abcg6-1 abcg20-1* mutant roots contrasts with the increased expression of most other suberin biosynthesis genes tested and could contribute to the reduced 22:0 fatty alcohol content of mutant suberin (Domergue et al., 2010; Vishwanath et al., 2013). *FAR1* and *FAR4* are induced by stress, as are several other suberin biosynthesis genes (Domergue et al., 2010; Geng et al., 2013), and their decreased expression in mutant roots could possibly reflect substrate-level negative feedback caused by decreased export of fatty alcohols in the mutant.

Additional ABCG proteins may also contribute to synthesis of suberin or other barrier polymers. Three additional closely related genes, *ABCG17*, *ABCG18*, and *ABCG19* (Figure 1A; Supplemental Figure 1), are adjacent on the genome to *ABCG16*. These three

genes were not expressed in roots, but *ABCG18* and *ABCG19* were strongly expressed in shoot epidermis (Mustroph et al., 2009) (Supplemental Table 1), and these might contribute to cutin synthesis. *ABCG10* and *ABCG23*, encoding ABCG proteins closely related to each other from a different clade, were also coexpressed with suberin biosynthesis genes (Supplemental Table 1). A pair of ABCG half-transporters in *Medicago truncatula* are closely related to the *Arabidopsis* clade studied here and localize to the periarbuscular membrane (Zhang et al., 2010). These may contribute to a barrier function or may transport a nutrient or signal essential for arbuscular mycorrhizal symbiosis.

Physiological Importance of Barriers

Mutants deficient in the Casparian strip lack a lignin barrier to apoplastic salt diffusion into the stele of the elongating part of the root (Naseer et al., 2012; Hosmani et al., 2013). In contrast, the *abcg2-1 abcg6-1 abcg20-1* and other suberin-deficient mutants had an intact Casparian strip but allowed salt movement to the stele in the more mature zone above the elongation zone affected in the Casparian strip mutants. Thus, the two barriers are important in complementary zones of the developing root. Endodermal cells may become more permeable as they mature, for example, if they express transporters that permit transcellular movement of salts and water (Steudle and Peterson, 1998). Still older mature roots undergoing secondary growth and periderm formation lose outer cell layers including the endodermis (Dolan et al., 1993; Dolan and Roberts, 1995; Baum et al., 2002; Matsumoto-Kitano et al., 2008). Thus, the Casparian lignin strip is a temporary barrier present in the youngest portions of roots, whereas suberin is required in older portions of roots, and to some degree replaces the Casparian strip. In such older roots, suberin might also impede apoplastic water and salt movement. That the Casparian strip and suberin may have some overlapping function is suggested by the increased induction of suberin biosynthesis in Casparian-strip-deficient mutants (Naseer et al., 2012; Hosmani et al., 2013) and by the increased phloroglucinol staining and autofluorescence in the central part of *abcg2-1 abcg6-1 abcg20-1* roots, indicating increased lignin or suberin aromatic subunit synthesis. It will be interesting to characterize plants deficient in both barriers and to explore the mechanisms by which plants modulate synthesis of extracellular barriers in response to drought or salt stress.

In addition to defects in extracellular barriers, *abcg2-1 abcg6-1 abcg20-1* mutants had morphological phenotypes that reveal putative developmental adjustments to altered water status. Mutant roots began secondary growth and periderm formation precociously, and mutant plants had fewer lateral roots than did wild-type plants. Known suberin-deficient mutants also had fewer lateral roots, although still more than *abcg2-1 abcg6-1 abcg20-1* plants. These results suggest that the lateral root defect is caused in part by suberin deficiency and that more complete suberin deficiency might reveal stronger phenotypes. Alternatively, ABCG2, ABCG6, and ABCG20 transporters may affect processes in addition to suberin biosynthesis, such as formation of other barrier compounds or export of signals.

Several possible regulatory pathways might cause these root architecture changes. Defective suberin barriers in mutant roots might lead to osmotic stress or water loss, thereby inducing responses by which wild-type plants adapt to drought conditions. Such responses might act through induction of ABA biosynthesis. However, mutant roots did not have a general increase in expression of ABA biosynthesis or response genes. Cytokinins stimulate secondary growth (Matsumoto-Kitano et al., 2008), and it is possible that mutant roots have increased cytokinin content or response. Defects in synthesis of very-long-chain fatty acids (including 20:0 and 22:0 fatty acids) and sphingolipids also cause increased cytokinin production and secondary growth (Roudier et al., 2010; Nobusawa et al., 2013), and some of the phenotypes seen in *abcg2-1 abcg6-1 abcg20-1* plants might therefore arise from altered fatty acid signaling. Lastly, sucrose uptake in the shoots of plants grown in tissue culture can stimulate auxin transport to the root and lateral root production (Macgregor et al., 2008; Lilley et al., 2012); therefore, decreased sucrose availability caused by low water potential might affect lateral root production. It is likely that altered root permeability affects development of many plants. For example, rice *abcg5/rcn1* mutants defective in a closely related transporter also have a defective suberin barrier and altered root and shoot architecture (Yasuno et al., 2009; Ureshi et al., 2012; Shiono et al., 2014).

METHODS

Plant Material, Growth Conditions, Phenotypic Analysis, and Hormone Treatments

All plant lines were in the Columbia (Col) ecotype. New Salk and GABI-Kat insertion lines used are summarized in Supplemental Figure 6 and were genotyped using primers listed in Supplemental Table 2. Unless otherwise stated, seeds were surface sterilized using 70% (v/v) ethanol and 0.5% (v/v) Triton X-100, plated on Murashige and Skoog (MS) salts (Murashige and Skoog, 1962) containing 1% (w/v) Suc and 0.8% (w/v) Phyto-agar (Research Products International) adjusted to pH 5.7 using KOH, and cold stratified for 2 to 3 d at 4°C before being transferred to controlled growth chambers at 22°C with 16-h-light and 8-h-dark conditions.

For seed germination assays, seeds were plated on MS+Suc plates with the indicated concentrations of ABA (Sigma-Aldrich) and kept at 4°C for 3 d before being moved to growth chambers. After 5 d of incubation, the seeds whose radical had emerged through the seed coat were scored as germinated. To assay the numbers of lateral roots in the presence or absence of IAA, seedlings were first grown for 5 d on vertically oriented plates in the absence of hormone and then transferred onto MS+Suc plates with the indicated concentrations of IAA. Lateral and adventitious roots were counted under a dissecting microscope or by staining with acetocarmine (Booker et al., 2010). To measure root and rosette leaf lengths, scanned images of seedlings or leaves were analyzed using Image J (Abramoff et al., 2004).

Promoter Fusions and Complementation of the *abcg2-1 abcg6-1 abcg20-1* Mutant

For promoter:GUS fusions, 1-kb sequences upstream of the start codon of *ABCG* genes were amplified using high fidelity Phusion polymerase (New England Biolabs) using primers listed in Supplemental Table 3 and then cloned into the *Sma*I restriction site of pBI101.2 (Clontech) to make the promoter:GUS fusion reporters. For complementation, a genomic region including 1.2 kb of putative promoter and the *ABCG2* coding region were amplified from genomic DNA of Col using primers listed in Supplemental Table 3 and cloned into the *Sma*I restriction site of

pCambia2300 (http://www.cambia.org/). Positive clones were identified by PCR and verified by sequencing. The Binary vector clones were introduced into *Agrobacterium tumefaciens* strain GV3101 pMP90 by electroporation and selecting kanamycin and gentamycin resistance. Wild-type Columbia or *abcg2-1 abcg6-1 abcg20-1* plants were then transformed by floral dip (Clough and Bent, 1998). T1 plants were selected on MS plates with 50 μg/ml kanamycin and lines segregating ~3:1 in the T2 generation were used for further analyses. X-Gluc staining was as described in (Jefferson, 1987). For wound assays, three-week-old plants were poked with a syringe and after 48 h stained with X-Gluc. For sections of stained flowers, tissue was processed as described by (Bomblies, 2002) with modifications described at http://www4.ncsu.edu/~rgfranks/research/protocols.html under "GUS staining."

Transient Expression in Tobacco for Subcellular Localization

Gene-specific primers (Supplemental Table 3) were used to amplify the cDNAs of *ABCG1*, *ABCG2*, *ABCG6*, *ABCG16*, and *ABCG20* without stop codons from flower cDNA using high-fidelity Phusion Taq polymerase (Invitrogen) and were cloned in pENTR/D-Topo (Invitrogen). Clones lacking the stop codon were used for LR recombination reactions with pGWB5 (Nakagawa et al., 2007) to generate the ABCG-GFP constructs. Expression clones were transformed into *Agrobacterium tumefaciens* strain GV3101. The *Agrobacterium* clones were grown overnight at 28°C, centrifuged at 3000 rpm for a few seconds to pellet down the cells, and washed twice with water. The washed pellet was then suspended in infiltration medium containing 10 mM $MgCl_2$, 10 mM MES, and 100 μM acetosyringone and were kept at room temperature for 2 h before being infiltrated into the abaxial side of *Nicotiana benthamiana* leaves using a 1-mL syringe. Infiltrated tobacco plants were grown under long days (16 h light:8 h dark). After 48 h of incubation, leaf sections were stained with 5 μM FM4-64 (Calbiochem, EMD Millipore) and observed under a confocal microscope with excitation at 488 nm and detection at 495 to 531 nm for GFP and excitation at 514 nm and detection at 601 to 759 nm for FM4-64.

Quantitative RT-PCR Analysis

Seedling, shoot, or root tissues were frozen in liquid N_2 and total RNA was extracted using RNeasy plant mini kits (Qiagen) according to the manufacturer's instructions. For real-time quantitative RT-PCR, cDNA was synthesized using the A3500 Reverse Transcription System (Promega) with random primers according to the manufacturer's instructions. Total RNA of 0.1 or 1 μg was used in a 20-μL volume reaction and incubated for 1 h at 42°C. The RT reaction mixture was diluted 10-fold, and 1 μL was used as a template in 10-μL PCR reaction using the 7900 HT Fast real-time PCR system from Applied Biosystems in standard mode with SYBR Green Master Mix (Applied Biosystems) following the manufacturer's protocol. The primers for transcript analysis were designed using the primer express software (Applied Biosystems) and are listed in Supplemental Table 3. The reactions were performed in triplicate and the products were checked by melting curve analysis. Values are averages of two or three biological replicates, normalized to the reference transcript *UBQ10*.

Microscopy

For Fluorol Yellow staining (Brundrett et al., 1991), seedlings were incubated in a freshly prepared solution of 0.01% (w/v) Fluorol Yellow (Santa Cruz Biotechnologies) in lactic acid (88.5%) with 1 g/mL chloral hydrate at 70°C for 1 h. The samples were washed two to three times with water and then observed under a Zeiss 710 DUO confocal laser scanning microscope (Zeiss) with yellow fluorescent protein filter with excitation at 514 nm and detection at 516 to 593 nm.

For Sudan Red staining, seedlings were incubated in a solution of Sudan Red 7B (Sigma-Aldrich) in polyethylene glycol 400:glycerol (90% PEG400:10% glycerol) as described by Brundrett et al. (1991), rinsed with water, and observed with a Leica MZ12.5 light microscope coupled to a digital camera.

For phloroglucinol staining, 7-d-old seedlings and hand sections of 1-month-old roots from soil-grown plants washed in distilled water were stained for 10 s in 1% phloroglucinol (Sigma-Aldrich) dissolved in 20% HCl (Jensen, 1962).

For Auramine-O staining (Dobritsa et al., 2009), anthers were placed on a microscope slide in a drop of 0.001% (w/v) Auramine-O (diluted from a stock 0.1% [w/v] in 50 mM Tris-HCl, pH 7.5) in 17% Suc. The anther was gently tapped with tweezers to release pollen. Pollen grains were allowed to sit in solution for 2 to 3 min before observation on a Zeiss 710 Duo Confocal microscope under fluorescein isothiocyanate settings with excitation at 488 nm and detection at 493 to 580 nm.

For Calcoflour staining, pollen grains were stained for 30 min in a drop of 1% (w/v) Calcofluor (Sigma-Aldrich) in water and observed by confocal microscopy with excitation at 405 nm and detection at 421 to 558 nm.

Transmission Electron Microscopy

Roots of 10-d-old seedlings were fixed in 2% glutaraldehyde 0.05 M sodium phosphate, pH 7.4, and stored at 4°C for several days before being processed. The roots were washed several times with 0.05 M sodium phosphate, pH 7.4, and then postfixed with 1% osmium tetraoxide in 0.05 M sodium phosphate, pH 7.4, for 1 h at room temperature. Samples were dehydrated in a graded ethanol series (30, 50, 75, 100, and 100%), followed by two changes in propylene oxide, and infiltrated with and embedded in epoxy resin PolyBed812 (Polysciences).

Dry seeds were rehydrated in 20 μM abscisic acid in water for 24 h at 4°C. Hydrated seeds were rinsed in water briefly and fixed for 24 h in 2% paraformaldehyde/2.5% glutaraldehyde in 0.1 M sodium cacodylate buffer, pH 7.4. To facilitate penetration of the processing reagents, the seed coats were nicked using a sharp scalpel. The seeds were postfixed with 1% osmium tetroxide/1.25% potassium ferrocyanide in 0.1 M sodium cacodylate buffer for 2 h at 4°C. Dehydration and resin infiltration steps were performed using a PELCO BioWave Pro microwave oven operating at 450 W (Ted Pella). Samples were dehydrated through an ascending series of acetone (10, 30, 50, 75, 100, 100, and 100%), and then infiltrated under vacuum in a microwave through a series of Spurr's resin:acetone solutions (Spurr's resin:acetone 1:2, 1:1, 2:1, and 100% Spurr's resin). Seeds were placed into embedding capsules filled with fresh Spurr's resin and polymerized for 16 h at 70°C.

Anthers were fixed in 4% paraformaldehyde and 2.5% glutaraldehyde in 0.05 M sodium cacodylate buffer, pH 6.9 (Quilichini et al., 2010), and stored at 4°C for several days before processing. Following several washes in 0.05 M sodium cacodylate buffer, the samples were postfixed in 1% osmium tetroxide in 0.05 M sodium cacodylate buffer for 1 h at room temperature. Samples were dehydrated in a graded ethanol series (30, 50, 75, 100, and 100%), followed by two changes in propylene oxide, and infiltrated with and embedded in Spurr's low viscosity epoxy resin (Polysciences).

For root, seed, and anther samples, 1-μm sections were cut and mounted on glass slides, stained with 1% Toluidine blue in 1% sodium borate, and viewed by light microscopy to select the region of interest for TEM. Ultrathin sections (70 nm) were cut using a diamond knife, mounted on 200 mesh copper grids (or 75 mesh Formvar-carbon coated copper grids, for seeds), and stained with 4% aqueous uranyl acetate and Reynold's lead citrate (Reynolds, 1963). Samples were observed using a LEO EM910 transmission electron microscope operating at 80 kV (Carl Zeiss Microscopy), and digital images were acquired using a Gatan Orius SC1000 CCD digital camera with Digital Micrograph 3.11.0 (Gatan).

Seed and Root Suberin Composition Analysis

Arabidopsis thaliana plants were germinated and grown on soil-vermiculite-perlite (2:1:1) for 7 weeks or on MS agar medium for 10 d. Suberin analyses

were performed on roots of 10-d-old seedlings, 7-week-old plants, and mature, dry seeds following the protocol described by Molina et al. (2006) with slight modifications. Seed (100 mg per replicate), mature root (150 mg per replicate), or 10-d-old root (15 to 20 mg per replicate) samples were quenched in hot isopropanol, ground with a polytron, and thoroughly delipidated with a series of solvent washes: isopropanol, chloroform:methanol (2:1, v/v), and chloroform:methanol (1:2, v/v) (~12 h each). Sodium methoxide-catalyzed depolymerization was performed on delipidated dry residues, with methyl heptadecanoate and pentadecanolactone as internal standards. Samples were evaporated to dryness under N_2 stream and derivatized with 100 μL, each, of pyridine and acetic anhydride at 60°C for 1 h. Derivatized samples were evaporated to dryness and dissolved in heptane:toluene (1:1). Acetyl derivatives of suberin monomers were analyzed by gas chromatography-mass spectrometry in an Agilent 6850 gas chromatograph equipped with an Agilent 5975 mass spectrometer. Splitless injection was used with a HP5-MS column (J&W Scientific; 30 m × 0.25 mm × 0.25-μm film thickness) with helium carrier gas at 2 mL min^{-1} and oven temperature programmed from 110 to 300°C at 10°C/min. Splitless injection was used and the mass spectrometer run in scan mode over 40 to 500 atomic mass units (electron impact ionization), with peaks quantified on the basis of their total ion current.

Root Wax Analysis

Waxes were extracted from roots of 7-week-old *Arabidopsis* plants (grown as described above) by dipping in $CHCl_3$ for 1 min (Li et al., 2007). After extraction, internal standards were added to $CHCl_3$ extracts, and extracts were evaporated to dryness under N_2. Internal standards included heptadecanoic acid (17:0), pentadecan-1-ol (15:0), tetracosane (C24), tridecanyl ferulate, and heptadecanyl coumarate (Kosma et al., 2012). Samples were derivatized with 100 μL pyridine and 100 μL *N,O*-bis (trimethylsilyl)trifluoroacetamide) at 110°C for 10 min. Derivatized samples were evaporated to dryness, dissolved in hexane, and analyzed on a Thermo Trace 1300 GC system coupled to an ISQ mass selective detector (EI). Gas chromatography analyses used a TG-5MS capillary column (Thermo Scientific; 30-m length, 0.25-mm i.d., and 0.25-μm film thickness) with helium carrier gas at 1.0 mL/min constant flow and temperature programmed from 150 to 325°C at 5°C/min and then held for an additional 10 min at 325°C. Split mode (5:1 ratio, 310°C injector temperature) was used and the mass spectrometer run in scan mode over 40 to 650 atomic mass units (electron impact ionization), with peaks quantified on the basis of their total ion current.

Seed Coat and Root Permeability Assays

For seed coat permeability tests, dry seeds were incubated in the dark in an aqueous solution of 1% (w/v) tetrazolium red (2,3,5-triphenyltetrazolium; Sigma-Aldrich) at 30°C for 8 to 48 h and then washed with water before imaging (Debeaujon et al., 2000). Root hydrostatic and osmotic hydraulic conductivity assays were performed as described (Ranathunge and Schreiber, 2011) using WinRhizo software to measure root surface area (Bouma et al., 2000). For PI permeability assays, 5-d-old seedlings were stained with 10 μM PI in darkness for 10 min and then washed two to three times with water before being observed under a Zeiss 710 Duo Confocal microscope (Lee et al., 2013). PI was detected with excitation at 560 nm and detection at 566 to 646 nm, and autofluorescence was detected with standard eYFP filter with excitation at 405 nm and detection at 416 to 528 nm.

Sequence Alignment and Phylogeny

For making the phylogenetic tree, the ABCG protein sequences were submitted to http://www.phylogeny.fr/ (Dereeper et al., 2008), which uses MUSCLE for multiple sequence alignment (Edgar, 2004), PhyML for phylogeny (Guindon et al., 2005), and TreeDyn for tree drawing (Chevenet et al., 2006).

Accession Numbers

Genes used in this work have the following Arabidopsis Genome Initiative designations: *ABCG1*, At2g39350; *ABCG2*, At2g37360; *ABCG6*, At5g13580; *ABCG16*, At3g55090; *ABCG17*, At3g55100; *ABCG18*, At3g55110; *ABCG19*, At3g55130; *ABCG20*, At3g53510; *GPAT5*, At3g11430; *FAR1*, At4g15090; *FAR4*, At3g44540; *FAR5*, At3g44550; *CYP86B1*, At5g23190; *CYP86A1*, At5g58860; *ASFT*, At5g41040; *MYB96*, *At5g62470*; *RAB18*, At5g66400; *COR47*, At1g20440, *NCED9*, At1g78390; *NCED3*, At3g14440; *NCED1*, At3g63520; *ABA1*, At5g67030; *ABA2*, At1g52340; *ABA3*, At1g16540; *AAO3*, At2g27510; and *CYP707A4*, At3g19270.

Supplemental Data

The following materials are available in the online version of this article and have also been deposited in the DRYAD repository under accession number http://dx.doi.org/10.5061/dryad.1hn66.

Supplemental Figure 1. Sequence Alignment of ABCG Proteins.

Supplemental Figure 2. Subcellular Localization of ABCG Proteins.

Supplemental Figure 3. X-Gluc Staining of Plants with P_{ABCG}:*GUS* Reporter Genes.

Supplemental Figure 4. Expression of *ABCG* Genes and Root Suberin Staining.

Supplemental Figure 5. *ABCG* Expression in Seeds.

Supplemental Figure 6. T-DNA Insertion Alleles of *ABCG* Genes.

Supplemental Figure 7. Seed Coat Permeability of Suberin-Deficient Mutants and Characterization of *abcg2-2 abcg6-2 abcg20-2* Phenotypes.

Supplemental Figure 8. Rescue of *abcg2-1 abcg6-1 abcg20-1* Triple Mutant Phenotypes by a Genomic *ABCG2* Gene Construct.

Supplemental Figure 9. Propidium Iodide Permeability Assays.

Supplemental Figure 10. Microscopy of Mature Roots from Soil-Grown Plants.

Supplemental Figure 11. TEM of Wild-Type and *abcg2-1 abcg6-1 abcg20-1* Seed Coats.

Supplemental Figure 12. Suberin Monomer Composition of Suberin from Wild Type and *abcg2-1 abcg6-1 abcg20-1*.

Supplemental Figure 13. Suberin Monomer Composition of Suberin from Roots of 10-d-Old Plants.

Supplemental Figure 14. Suberin Monomer Composition of Suberin from Roots of 7-Week-Old Plants of Single and Double Mutants.

Supplemental Figure 15. Lateral Roots in *abcg* and Suberin-Deficient Mutants.

Supplemental Figure 16. Rosettes of Col and *abcg2-1 abcg6-1 abcg20-1* Plants Grown in Soil.

Supplemental Figure 17. Phenotypes of *abcg1-2 abcg16-2* Plants.

Supplemental Table 1. Proportions of Collapsed Pollen from *abcg1-2* and *abcg16-2* Single and Double Mutant Plants.

Supplemental Table 2. Segregation of Genotypes among Progeny of *ABCG1/abcg1-2 ABCG16/abcg16-2* Plants.

Supplemental Table 3. Primers Used in This Work.

Supplemental Data Set 1. Alignments Used to Generate the Phylogeny Presented in Figure 1A.

Supplemental Data Set 2. Translatome Data for Suberin Biosynthesis and *ABCG* Genes in Different Root and Shoot Cell Types.

Supplemental Data Set 3. Expression of NaCl-Inducible Suberin Biosynthesis and *ABCG* Genes in Selected Root Cell Types.

ACKNOWLEDGMENTS

This work was supported by National Science Foundation Grant IOS-1147045 to J.W.R. and Punita Nagpal and by an NSERC-Discovery grant to I.M. We thank Victoria Madden for help with TEM; Tony Perdue for help with confocal microscopy; Saurabh Habibi for running mass spectrometry assays; and David Salt, Niko Geldner, and José Dinneny for seeds.

AUTHOR CONTRIBUTIONS

V.Y., I.M., K.R., and J.W.R. designed the research. V.Y., I.M., K.R., and I.Q.C. performed research. V.Y., I.M., K.R., S.J.R., and J.W.R. analyzed data. V.Y., I.M., and J.W.R. wrote the article.

Received June 19, 2014; revised August 2, 2014; accepted August 19, 2014; published September 12, 2014.

REFERENCES

Abramoff, M.D., Magelhaes, P.J., and Ram, S.J. (2004). Image Processing with ImageJ. Biophotonics International **11:** 36–42.

Alejandro, S., Lee, Y., Tohge, T., Sudre, D., Osorio, S., Park, J., Bovet, L., Lee, Y., Geldner, N., Fernie, A.R., and Martinoia, E. (2012). AtABCG29 is a monolignol transporter involved in lignin biosynthesis. Curr. Biol. **22:** 1207–1212.

Ariizumi, T., Hatakeyama, K., Hinata, K., Sato, S., Kato, T., Tabata, S., and Toriyama, K. (2003). A novel male-sterile mutant of *Arabidopsis thaliana*, faceless pollen-1, produces pollen with a smooth surface and an acetolysis-sensitive exine. Plant Mol. Biol. **53:** 107–116.

Ariizumi, T., and Toriyama, K. (2011). Genetic regulation of sporopollenin synthesis and pollen exine development. Annu. Rev. Plant Biol. **62:** 437–460.

Baum, S.F., Dubrovsky, J.G., and Rost, T.L. (2002). Apical organization and maturation of the cortex and vascular cylinder in *Arabidopsis thaliana* (Brassicaceae) roots. Am. J. Bot. **89:** 908–920.

Baxter, I., Hosmani, P.S., Rus, A., Lahner, B., Borevitz, J.O., Muthukumar, B., Mickelbart, M.V., Schreiber, L., Franke, R.B., and Salt, D.E. (2009). Root suberin forms an extracellular barrier that affects water relations and mineral nutrition in Arabidopsis. PLoS Genet. **5:** e1000492.

Beisson, F., Li-Beisson, Y., and Pollard, M. (2012). Solving the puzzles of cutin and suberin polymer biosynthesis. Curr. Opin. Plant Biol. **15:** 329–337.

Beisson, F., Li, Y., Bonaventure, G., Pollard, M., and Ohlrogge, J.B. (2007). The acyltransferase GPAT5 is required for the synthesis of suberin in seed coat and root of Arabidopsis. Plant Cell **19:** 351–368.

Bernards, M.A. (2002). Demystifying suberin. Can. J. Bot. **80:** 227–240.

Bessire, M., Borel, S., Fabre, G., Carraça, L., Efremova, N., Yephremov, A., Cao, Y., Jetter, R., Jacquat, A.C., Métraux, J.P., and Nawrath, C. (2011). A member of the PLEIOTROPIC DRUG RESISTANCE family of ATP binding cassette transporters is required for the formation of a functional cuticle in Arabidopsis. Plant Cell **23:** 1958–1970.

Bird, D., Beisson, F., Brigham, A., Shin, J., Greer, S., Jetter, R., Kunst, L., Wu, X., Yephremov, A., and Samuels, L. (2007). Characterization of Arabidopsis ABCG11/WBC11, an ATP binding cassette (ABC) transporter that is required for cuticular lipid secretion. Plant J. **52:** 485–498.

Blackmore, S., Wortley, A.H., Skvarla, J.J., and Rowley, J.R. (2007). Pollen wall development in flowering plants. New Phytol. **174:** 483–498.

Bomblies, K. (2002). Whole-mount GUS staining. In Arabidopsis: A Laboratory Manual, D. Weigel and J. Glazebrook, eds (Cold Spring Harbor, NY: Cold Spring Harbor Laboratory Press), pp. 243–248.

Booker, K.S., Schwarz, J., Garrett, M.B., and Jones, A.M. (2010). Glucose attenuation of auxin-mediated bimodality in lateral root formation is partly coupled by the heterotrimeric G protein complex. PLoS ONE **5:** 5.

Bouma, T.J., Nielson, K.L., and Koutsaal, B. (2000). Sample preparation and scanning protocol for computerised analysis of root length and diameter. Plant Soil **218:** 185–196.

Brundrett, M.C., Kendrick, B., and Peterson, C.A. (1991). Efficient lipid staining in plant material with sudan red 7B or fluorol [correction of fluoral] yellow 088 in polyethylene glycol-glycerol. Biotech. Histochem. **66:** 111–116.

Chevenet, F., Brun, C., Bañuls, A.L., Jacq, B., and Christen, R. (2006). TreeDyn: towards dynamic graphics and annotations for analyses of trees. BMC Bioinformatics **7:** 439.

Choi, H., Ohyama, K., Kim, Y.Y., Jin, J.Y., Lee, S.B., Yamaoka, Y., Muranaka, T., Suh, M.C., Fujioka, S., and Lee, Y. (2014). The role of Arabidopsis ABCG9 and ABCG31 ATP binding cassette transporters in pollen fitness and the deposition of steryl glycosides on the pollen coat. Plant Cell **26:** 310–324.

Clough, S.J., and Bent, A.F. (1998). Floral dip: a simplified method for Agrobacterium-mediated transformation of *Arabidopsis thaliana*. Plant J. **16:** 735–743.

Comas, L.H., Becker, S.R., Cruz, V.M.V., Byrne, P.F., and Dierig, D.A. (2013). Root traits contributing to plant productivity under drought. Front. Plant Sci. **4:** 442.

Compagnon, V., Diehl, P., Benveniste, I., Meyer, D., Schaller, H., Schreiber, L., Franke, R., and Pinot, F. (2009). CYP86B1 is required for very long chain omega-hydroxyacid and alpha, omega-dicarboxylic acid synthesis in root and seed suberin polyester. Plant Physiol. **150:** 1831–1843.

de Azevedo Souza, C., Kim, S.S., Koch, S., Kienow, L., Schneider, K., McKim, S.M., Haughn, G.W., Kombrink, E., and Douglas, C.J. (2009). A novel fatty Acyl-CoA synthetase is required for pollen development and sporopollenin biosynthesis in Arabidopsis. Plant Cell **21:** 507–525.

Debeaujon, I., Léon-Kloosterziel, K.M., and Koornneef, M. (2000). Influence of the testa on seed dormancy, germination, and longevity in Arabidopsis. Plant Physiol. **122:** 403–414.

Dereeper, A., Guignon, V., Blanc, G., Audic, S., Buffet, S., Chevenet, F., Dufayard, J.F., Guindon, S., Lefort, V., Lescot, M., Claverie, J.M., and Gascuel, O. (2008). Phylogeny.fr: robust phylogenetic analysis for the non-specialist. Nucleic Acids Res. **36:** W465-W469.

Dickinson, H.G., and Heslop-Harrison, J. (1968). Common mode of deposition for the sporopollenin of sexine and nexine. Nature **220:** 926–927.

Dobritsa, A.A., Geanconteri, A., Shrestha, J., Carlson, A., Kooyers, N., Coerper, D., Urbanczyk-Wochniak, E., Bench, B.J., Sumner, L.W., Swanson, R., and Preuss, D. (2011). A large-scale genetic screen in Arabidopsis to identify genes involved in pollen exine production. Plant Physiol. **157:** 947–970.

Dobritsa, A.A., Shrestha, J., Morant, M., Pinot, F., Matsuno, M., Swanson, R., Møller, B.L., and Preuss, D. (2009). CYP704B1 is a long-chain fatty acid omega-hydroxylase essential for sporopollenin synthesis in pollen of Arabidopsis. Plant Physiol. **151:** 574–589.

Dolan, L., and Roberts, K. (1995). Secondary thickening in roots of *Arabidopsis thaliana*: Anatomy and cell-surface changes. New Phytol. **131:** 121–128.

Dolan, L., Janmaat, K., Willemsen, V., Linstead, P., Poethig, S., Roberts, K., and Scheres, B. (1993). Cellular organisation of the *Arabidopsis thaliana* root. Development **119:** 71–84.

Domergue, F., Vishwanath, S.J., Joubès, J., Ono, J., Lee, J.A., Bourdon, M., Alhattab, R., Lowe, C., Pascal, S., Lessire, R., and Rowland, O. (2010). Three Arabidopsis fatty acyl-coenzyme A reductases, FAR1, FAR4, and FAR5, generate primary fatty alcohols associated with suberin deposition. Plant Physiol. **153:** 1539–1554.

Duan, L., Dietrich, D., Ng, C.H., Chan, P.M., Bhalerao, R., Bennett, M.J., and Dinneny, J.R. (2013). Endodermal ABA signaling promotes lateral root quiescence during salt stress in Arabidopsis seedlings. Plant Cell **25:** 324–341.

Edgar, R.C. (2004). MUSCLE: multiple sequence alignment with high accuracy and high throughput. Nucleic Acids Res. **32:** 1792–1797.

Franke, R., Höfer, R., Briesen, I., Emsermann, M., Efremova, N., Yephremov, A., and Schreiber, L. (2009). The DAISY gene from Arabidopsis encodes a fatty acid elongase condensing enzyme involved in the biosynthesis of aliphatic suberin in roots and the chalaza-micropyle region of seeds. Plant J. **57:** 80–95.

Gambetta, G.A., Fei, J., Rost, T.L., Knipfer, T., Matthews, M.A., Shackel, K.A., Walker, M.A., and McElrone, A.J. (2013). Water uptake along the length of grapevine fine roots: developmental anatomy, tissue-specific aquaporin expression, and pathways of water transport. Plant Physiol. **163:** 1254–1265.

Geng, Y., Wu, R., Wee, C.W., Xie, F., Wei, X., Chan, P.M., Tham, C., Duan, L., and Dinneny, J.R. (2013). A spatio-temporal understanding of growth regulation during the salt stress response in Arabidopsis. Plant Cell **25:** 2132–2154.

Gou, J.Y., Yu, X.H., and Liu, C.J. (2009). A hydroxycinnamoyltransferase responsible for synthesizing suberin aromatics in Arabidopsis. Proc. Natl. Acad. Sci. USA **106:** 18855–18860.

Guindon, S., Lethiec, F., Duroux, P., and Gascuel, O. (2005). PHYML Online—a web server for fast maximum likelihood-based phylogenetic inference. Nucleic Acids Res. **33:** W557–W559.

Higgins, C.F., and Linton, K.J. (2004). The ATP switch model for ABC transporters. Nat. Struct. Mol. Biol. **11:** 918–926.

Höfer, R., Briesen, I., Beck, M., Pinot, F., Schreiber, L., and Franke, R. (2008). The Arabidopsis cytochrome P450 CYP86A1 encodes a fatty acid omega-hydroxylase involved in suberin monomer biosynthesis. J. Exp. Bot. **59:** 2347–2360.

Hosmani, P.S., Kamiya, T., Danku, J., Naseer, S., Geldner, N., Guerinot, M.L., and Salt, D.E. (2013). Dirigent domain-containing protein is part of the machinery required for formation of the lignin-based Casparian strip in the root. Proc. Natl. Acad. Sci. USA **110:** 14498–14503.

Jefferson, R.A. (1987). Assaying chimeric genes in plants: The GUS gene fusion system. Plant Mol. Biol. Rep. **5:** 387–405.

Jensen, W.A. (1962). Botanical Histochemistry. (San Francisco, CA: W.H. Freeman and Company).

Kang, J., Hwang, J.U., Lee, M., Kim, Y.Y., Assmann, S.M., Martinoia, E., and Lee, Y. (2010). PDR-type ABC transporter mediates cellular uptake of the phytohormone abscisic acid. Proc. Natl. Acad. Sci. USA **107:** 2355–2360.

Ko, D., et al. (2014). Arabidopsis ABCG14 is essential for the root-to-shoot translocation of cytokinin. Proc. Natl. Acad. Sci. USA **111:** 7150–7155.

Kosma, D.K., Molina, I., Ohlrogge, J.B., and Pollard, M. (2012). Identification of an Arabidopsis fatty alcohol:caffeoyl-coenzyme A acyltransferase required for the synthesis of alkyl hydroxycinnamates in root waxes. Plant Physiol. **160:** 237–248.

Kretzschmar, T., Kohlen, W., Sasse, J., Borghi, L., Schlegel, M., Bachelier, J.B., Reinhardt, D., Bours, R., Bouwmeester, H.J., and Martinoia, E. (2012). A petunia ABC protein controls strigolactone-dependent symbiotic signalling and branching. Nature **483:** 341–344.

Kuromori, T., Ito, T., Sugimoto, E., and Shinozaki, K. (2011). Arabidopsis mutant of AtABCG26, an ABC transporter gene, is defective in pollen maturation. J. Plant Physiol. **168:** 2001–2005.

Kuromori, T., Miyaji, T., Yabuuchi, H., Shimizu, H., Sugimoto, E., Kamiya, A., Moriyama, Y., and Shinozaki, K. (2010). ABC transporter AtABCG25 is involved in abscisic acid transport and responses. Proc. Natl. Acad. Sci. USA **107:** 2361–2366.

Le, B.H., et al. (2010). Global analysis of gene activity during Arabidopsis seed development and identification of seed-specific transcription factors. Proc. Natl. Acad. Sci. USA **107:** 8063–8070.

Le Hir, R., Sorin, C., Chakraborti, D., Moritz, T., Schaller, H., Tellier, F., Robert, S., Morin, H., Bako, L., and Bellini, C. (2013). ABCG9, ABCG11 and ABCG14 ABC transporters are required for vascular development in Arabidopsis. Plant J. **76:** 811–824.

Lee, I., Ambaru, B., Thakkar, P., Marcotte, E.M., and Rhee, S.Y. (2010). Rational association of genes with traits using a genome-scale gene network for *Arabidopsis thaliana*. Nat. Biotechnol. **28:** 149–156.

Lee, S.B., Jung, S.J., Go, Y.S., Kim, H.U., Kim, J.K., Cho, H.J., Park, O.K., and Suh, M.C. (2009). Two Arabidopsis 3-ketoacyl CoA synthase genes, KCS20 and KCS2/DAISY, are functionally redundant in cuticular wax and root suberin biosynthesis, but differentially controlled by osmotic stress. Plant J. **60:** 462–475.

Lee, Y., Rubio, M.C., Alassimone, J., and Geldner, N. (2013). A mechanism for localized lignin deposition in the endodermis. Cell **153:** 402–412.

Li, Y., Beisson, F., Koo, A.J., Molina, I., Pollard, M., and Ohlrogge, J. (2007). Identification of acyltransferases required for cutin biosynthesis and production of cutin with suberin-like monomers. Proc. Natl. Acad. Sci. USA **104:** 18339–18344.

Lilley, J.L., Gee, C.W., Sairanen, I., Ljung, K., and Nemhauser, J.L. (2012). An endogenous carbon-sensing pathway triggers increased auxin flux and hypocotyl elongation. Plant Physiol. **160:** 2261–2270.

Lou, Y., Xu, X.F., Zhu, J., Gu, J.N., Blackmore, S., and Yang, Z.N. (2014). The tapetal AHL family protein TEK determines nexine formation in the pollen wall. Nat. Commun. **5:** 3855.

Luo, B., Xue, X.Y., Hu, W.L., Wang, L.J., and Chen, X.Y. (2007). An ABC transporter gene of *Arabidopsis thaliana*, AtWBC11, is involved in cuticle development and prevention of organ fusion. Plant Cell Physiol. **48:** 1790–1802.

Macgregor, D.R., Deak, K.I., Ingram, P.A., and Malamy, J.E. (2008). Root system architecture in Arabidopsis grown in culture is regulated by sucrose uptake in the aerial tissues. Plant Cell **20:** 2643–2660.

Matsumoto-Kitano, M., Kusumoto, T., Tarkowski, P., Kinoshita-Tsujimura, K., Václavíková, K., Miyawaki, K., and Kakimoto, T. (2008). Cytokinins are central regulators of cambial activity. Proc. Natl. Acad. Sci. USA **105:** 20027–20031.

McFarlane, H.E., Shin, J.J., Bird, D.A., and Samuels, A.L. (2010). Arabidopsis ABCG transporters, which are required for export of diverse cuticular lipids, dimerize in different combinations. Plant Cell **22:** 3066–3075.

Molina, I., Bonaventure, G., Ohlrogge, J., and Pollard, M. (2006). The lipid polyester composition of *Arabidopsis thaliana* and *Brassica napus* seeds. Phytochemistry **67:** 2597–2610.

Molina, I., Li-Beisson, Y., Beisson, F., Ohlrogge, J.B., and Pollard, M. (2009). Identification of an Arabidopsis feruloyl-coenzyme A transferase required for suberin synthesis. Plant Physiol. **151:** 1317–1328.

Morant, M., Jørgensen, K., Schaller, H., Pinot, F., Møller, B.L., Werck-Reichhart, D., and Bak, S. (2007). CYP703 is an ancient cytochrome P450 in land plants catalyzing in-chain hydroxylation of lauric acid to provide building blocks for sporopollenin synthesis in pollen. Plant Cell **19:** 1473–1487.

Murashige, T., and Skoog, F. (1962). A revised medium for rapid growth and bioassays with tobacco tissue cultures. Physiol. Plant. **15:** 473–497.

Mustroph, A., Zanetti, M.E., Jang, C.J., Holtan, H.E., Repetti, P.P., Galbraith, D.W., Girke, T., and Bailey-Serres, J. (2009). Profiling translatomes of discrete cell populations resolves altered cellular priorities during hypoxia in Arabidopsis. Proc. Natl. Acad. Sci. USA **106:** 18843–18848.

Nakagawa, T., Kurose, T., Hino, T., Tanaka, K., Kawamukai, M., Niwa, Y., Toyooka, K., Matsuoka, K., Jinbo, T., and Kimura, T. (2007). Development of series of gateway binary vectors, pGWBs, for realizing efficient construction of fusion genes for plant transformation. J. Biosci. Bioeng. **104:** 34–41.

Naseer, S., Lee, Y., Lapierre, C., Franke, R., Nawrath, C., and Geldner, N. (2012). Casparian strip diffusion barrier in Arabidopsis is made of a lignin polymer without suberin. Proc. Natl. Acad. Sci. USA **109:** 10101–10106.

Nawrath, C., Schreiber, L., Franke, R.B., Geldner, N., Reina-Pinto, J.J., and Kunst, L. (2013). Apoplastic diffusion barriers in Arabidopsis. The Arabidopsis Book **11:** e0167, doi/10.1199/tab.0167.

Nobusawa, T., Okushima, Y., Nagata, N., Kojima, M., Sakakibara, H., and Umeda, M. (2013). Synthesis of very-long-chain fatty acids in the epidermis controls plant organ growth by restricting cell proliferation. PLoS Biol. **11:** e1001531.

Obayashi, T., Okamura, Y., Ito, S., Tadaka, S., Aoki, Y., Shirota, M., and Kinoshita, K. (2014). ATTED-II in 2014: evaluation of gene coexpression in agriculturally important plants. Plant Cell Physiol. **55:** e6.

Panikashvili, D., Shi, J.X., Schreiber, L., and Aharoni, A. (2011). The Arabidopsis ABCG13 transporter is required for flower cuticle secretion and patterning of the petal epidermis. New Phytol. **190:** 113–124.

Panikashvili, D., Shi, J.X., Bocobza, S., Franke, R.B., Schreiber, L., and Aharoni, A. (2010). The Arabidopsis DSO/ABCG11 transporter affects cutin metabolism in reproductive organs and suberin in roots. Mol. Plant **3:** 563–575.

Panikashvili, D., Savaldi-Goldstein, S., Mandel, T., Yifhar, T., Franke, R.B., Höfer, R., Schreiber, L., Chory, J., and Aharoni, A. (2007). The Arabidopsis DESPERADO/AtWBC11 transporter is required for cutin and wax secretion. Plant Physiol. **145:** 1345–1360.

Pighin, J.A., Zheng, H., Balakshin, L.J., Goodman, I.P., Western, T.L., Jetter, R., Kunst, L., and Samuels, A.L. (2004). Plant cuticular lipid export requires an ABC transporter. Science **306:** 702–704.

Qin, P., Tu, B., Wang, Y., Deng, L., Quilichini, T.D., Li, T., Wang, H., Ma, B., and Li, S. (2013). ABCG15 encodes an ABC transporter protein, and is essential for post-meiotic anther and pollen exine development in rice. Plant Cell Physiol. **54:** 138–154.

Quilichini, T.D., Grienenberger, E., and Douglas, C.J. (2014). The biosynthesis, composition and assembly of the outer pollen wall: A tough case to crack. Phytochemistry, in press.

Quilichini, T.D., Friedmann, M.C., Samuels, A.L., and Douglas, C.J. (2010). ATP-binding cassette transporter G26 is required for male fertility and pollen exine formation in Arabidopsis. Plant Physiol. **154:** 678–690.

Ranathunge, K., and Schreiber, L. (2011). Water and solute permeabilities of Arabidopsis roots in relation to the amount and composition of aliphatic suberin. J. Exp. Bot. **62:** 1961–1974.

Reynolds, E.S. (1963). The use of lead citrate at high pH as an electron-opaque stain in electron microscopy. J. Cell Biol. **17:** 208–212.

Roudier, F., et al. (2010). Very-long-chain fatty acids are involved in polar auxin transport and developmental patterning in Arabidopsis. Plant Cell **22:** 364–375.

Ruzicka, K., et al. (2010). Arabidopsis PIS1 encodes the ABCG37 transporter of auxinic compounds including the auxin precursor indole-3-butyric acid. Proc. Natl. Acad. Sci. USA **107:** 10749–10753.

Sánchez-Fernández, R., Davies, T.G., Coleman, J.O., and Rea, P.A. (2001). The *Arabidopsis thaliana* ABC protein superfamily, a complete inventory. J. Biol. Chem. **276:** 30231–30244.

Schmutz, A., Buchala, A.J., and Ryser, U. (1996). Changing the dimensions of suberin lamellae of green cotton fibers with a specific inhibitor of the endoplasmic reticulum-associated fatty acid elongases. Plant Physiol. **110:** 403–411.

Schreiber, L. (2010). Transport barriers made of cutin, suberin and associated waxes. Trends Plant Sci. **15:** 546–553.

Serra, O., Hohn, C., Franke, R., Prat, S., Molinas, M., and Figueras, M. (2010). A feruloyl transferase involved in the biosynthesis of suberin and suberin-associated wax is required for maturation and sealing properties of potato periderm. Plant J. **62:** 277–290.

Serra, O., Soler, M., Hohn, C., Sauveplane, V., Pinot, F., Franke, R., Schreiber, L., Prat, S., Molinas, M., and Figueras, M. (2009). CYP86A33-targeted gene silencing in potato tuber alters suberin composition, distorts suberin lamellae, and impairs the periderm's water barrier function. Plant Physiol. **149:** 1050–1060.

Shiono, K., et al. (2014). RCN1/OsABCG5, an ATP-binding cassette (ABC) transporter, is required for hypodermal suberization of roots in rice (Oryza sativa). Plant J., in press.

Smyth, D.R., Bowman, J.L., and Meyerowitz, E.M. (1990). Early flower development in Arabidopsis. Plant Cell **2:** 755–767.

Steudle, E., and Peterson, C.A. (1998). How does water get through roots? J. Exp. Bot. **49:** 775–788.

Strader, L.C., and Bartel, B. (2009). The Arabidopsis PLEIOTROPIC DRUG RESISTANCE8/ABCG36 ATP binding cassette transporter modulates sensitivity to the auxin precursor indole-3-butyric acid. Plant Cell **21:** 1992–2007.

Ureshi, A.N., Matuda, S., Ohashi, E., Onishi, K., Takamure, I., and Kato, K. (2012). The rice RCN1/OsABCG5 mutation is associated with root development in response to nutrient shortage. Plant Root **6:** 28–35.

Verrier, P.J., et al. (2008). Plant ABC proteins—a unified nomenclature and updated inventory. Trends Plant Sci. **13:** 151–159.

Vishwanath, S.J., Kosma, D.K., Pulsifer, I.P., Scandola, S., Pascal, S., Joubès, J., Dittrich-Domergue, F., Lessire, R., Rowland, O., and Domergue, F. (2013). Suberin-associated fatty alcohols in Arabidopsis: distributions in roots and contributions to seed coat barrier properties. Plant Physiol. **163:** 1118–1132.

Weber, M., and Ulrich, S. (2010). The endexine: a frequently overlooked pollen wall layer and a simple method for detection. Grana **49:** 83–90.

Wilson, Z.A., Song, J., Taylor, B., and Yang, C. (2011). The final split: the regulation of anther dehiscence. J. Exp. Bot. **62:** 1633–1649.

Wood, P.J. (1980). Specificity in the interaction of direct dyes with polysaccharides. Carbohydr. Res. **85:** 271–287.

Xiong, L., Wang, R.G., Mao, G., and Koczan, J.M. (2006). Identification of drought tolerance determinants by genetic analysis of root response to drought stress and abscisic acid. Plant Physiol. **142:** 1065–1074.

Yasuno, N., Takamure, I., Kidou, S., Tokuji, Y., Ureshi, A.N., Funabiki, A., Ashikaga, K., Yamanouchi, U., Yano, M., and Kato, K. (2009). Rice shoot branching requires an ATP-binding cassette subfamily G protein. New Phytol. **182:** 91–101.

Zhang, K., Novak, O., Wei, Z., Gou, M., Zhang, X., Yu, Y., Yang, H., Cai, Y., Strnad, M., and Liu, C.J. (2014). Arabidopsis ABCG14 protein controls the acropetal translocation of root-synthesized cytokinins. Nat. Commun. **5:** 3274.

Zhang, Q., Blaylock, L.A., and Harrison, M.J. (2010). Two *Medicago truncatula* half-ABC transporters are essential for arbuscule development in arbuscular mycorrhizal symbiosis. Plant Cell **22:** 1483–1497.

Zolla, G., Heimer, Y.M., and Barak, S. (2010). Mild salinity stimulates a stress-induced morphogenic response in *Arabidopsis thaliana* roots. J. Exp. Bot. **61:** 211–224.

ABCG Transporters Are Required for Suberin and Pollen Wall Extracellular Barriers in *Arabidopsis*

Vandana Yadav, Isabel Molina, Kosala Ranathunge, Indira Queralta Castillo, Steven J. Rothstein and Jason W. Reed

Plant Cell 2014;26;3569-3588; originally published online September 12, 2014;
DOI 10.1105/tpc.114.129049